ACID FRACTURE AND FRACTURE CONDUCTIVITY STUDY OF FIELD ROCK SAMPLES

A Thesis

by

JARROD THOMAS UNDERWOOD

Submitted to the Office of Graduate and Professional Studies of
Texas A&M University
in partial fulfillment of the requirements for the degree of

MASTER OF SCIENCE

Chair of Committee,	Ding Zhu
Committee Members,	A. Daniel Hill
	Victor Ugaz
Head of Department,	A. Daniel Hill

December 2013

Major Subject: Petroleum Engineering

ABSTRACT

Acid fracturing is a well stimulation strategy designed to increase the productivity of a producing well. The parameters of acid fracturing and the effects of acid interaction on specific rock samples can be studied experimentally. Acid injection data and fracture conductivity measurements obtained in the research presented in this thesis yielded results that qualified and quantified the impact of a specific acid system on rock samples of varying acid solubility.

Six rock samples from a carbonate reservoir were labeled A through F to protect proprietary information included in this research. A 2% potassium chloride solution was used for the acid system and fracture conductivity measurements to prevent clay swelling. Injection temperature, contact time, and injection rate were designed to simulate field treatment conditions. The effects of a chelating agent on fracture conductivity were also studied.

Before and after images of the rock samples indicated that the effect of 15% hydrochloric acid on the samples was limited but correlated with the rock acid solubility. Samples E and F had a greater value of acid solubility and showed noticeable surface etching. Samples A, B, and C had lower values of acid solubility and did not show signs of surface etching. Sample D was of moderate acid solubility and showed minimal signs of surface etching. Fracture conductivity did not correlate directly with acid solubility, but likely was a function of inherent matrix permeability based on leak-off

measurements and fracture conductivity measurements. Finally, the fracture conductivity of Sample D increased after exposure to a chelating agent.

Commonly, acid fracture experimental studies are carried out with outcrop rock samples. The samples have more homogenous properties and without hydrocarbon content. In this study, cores from downhole formation were used. The original condition was preserved as much as possible to simulate real field situations. However, using field rock samples does present challenges not generally associated with outcrop rock samples.

Based on the information gathered from the work presented in this thesis, conclusions were drawn concerning the effectiveness of a 15% hydrochloric acid treatment in this formation and the challenges of using field rock samples.

DEDICATION

To the smartest men I know. One showed me how to be an Engineer; the other showed me how to be a man of God. Grandpa Bro and Grandpa Reeves, I love you both.

ACKNOWLEDGEMENTS

I would first like to thank Dr. Zhu for allowing me to research in the acid fracturing group and giving me the tools I needed to complete this research. Who would have known that a five-minute chat about a trip to Malaysia would spark such an eventful journey?

I would like to thank Dr. Hill for serving on my research committee and offering wisdom and experience at a moments notice.

I would also to thank Dr. Ugaz for serving on my committee and for being an email away to meet up and council me on graduate studies, engineering, and life.

Thank you Ali Almomen and Andrea Peñaloza for letting me watch and learn how to load the cell, inject acid, measure fracture conductivity, and maintain focus.

And finally, thank to my mother and father for their encouragement from the first day of Pre-school until the day I walk for my Masters degree graduation.

NOMENCLATURE

A	Cross Sectional Area of Flow, [L^2]
C_1	Nierode and Kruk Correlation Parameter
C_2	Nierode and Kruk Correlation Parameter
DREC	Dissolved Rock Equivalent Conductivity, [L^3]
k	Permeability, [L^2]
k_fw	Fracture Conductivity, [L^3]
L	Thickness of Porous Material, [L]
ΔP	Pressure Drop Across Porous Material, $\left[\frac{\mathrm{m}}{\mathrm{L}*\mathrm{t}^2}\right]$
σ_c	Closure Stress, $\left[\frac{\mathrm{m}}{\mathrm{L}*\mathrm{t}^2}\right]$
Q	Flowrate, $\left[\frac{L^3}{t}\right]$
μ	Viscosity, $\left[\frac{\mathrm{m}}{\mathrm{L}*\mathrm{t}}\right]$

TABLE OF CONTENTS

Page

ABSTRACT ii

DEDICATION iv

ACKNOWLEDGEMENTS v

NOMENCLATURE vi

TABLE OF CONTENTS vii

LIST OF TABLES xi

CHAPTER I INTRODUCTION AND LITERATURE REVIEW 1

- Introduction 1
- Literature Review 3
- Research Objectives 6

CHAPTER II SET-UP AND PROCEDURE 7

- Experimental Set-Up 7
- Experimental Procedure 12
- Conductivity Calculations 23

CHAPTER III EXPERIMENTAL RESULTS AND DISCUSSION 25

- SEM-EDX Analysis 25
- Acid Injection 30
- Fracture Conductivity 35
- Effects of Chelating Agent 37
- Comparison of Field Samples and Outcrop Samples 39

CHAPTER IV CONCLUSIONS AND RECOMMENDATIONS 44

- Conclusions 44
- Recommendations 45

REFERENCES 47

APPENDIX A PHOTOGRAPHS BEFORE AND AFTER ACID INJECTION 50

Sample A 50
Sample B.....52
Sample C.....54
Sample D 56
Sample E.....58
Sample F 60

APPENDIX B ACID FRACTURING SUPPLY LIST.....62

APPENDIX C DATA SHEETS.....64

Sample A 64
Sample B.....66
Sample C.....67
Sample D 69
Sample E.....71
Sample F 73

LIST OF FIGURES

Page

Figure 1: Fracture Formation in the Presence of Acid (After Pounik 2008).....2

Figure 2: Modified API Cell and Rock Samples.....7

Figure 3: Schematic of Acid Injection Apparatus (After Zou 2005) 9

Figure 4: Schematic of Conductivity Measurement Apparatus (After Zou 2005).....10

Figure 5: Profilometer Used to Determine Volume Removed.....11

Figure 6: Path of Profilometer Scan (After Melendez 2007) 11

Figure 7: Experimental Procedure Flowchart 12

Figure 8: Example of Removing Excess Tape from Rock Sample.....14

Figure 9: Application of Silicone Primer 15

Figure 10: Pouring Silicone at the Ends of the Rock Sample 16

Figure 11: Vacuum Pump Equipment.....17

Figure 12: Placement of Teflon Tape on Rock Sample 17

Figure 13: Placement of O-Rings Inside the Cell.....18

Figure 14: Cell Prepared for Acid Injection.....19

Figure 15: Cell Prepared for Fracture Conductivity Measurement.....22

Figure 16: Rock Sample for SEM/EDX Analysis.....25

Figure 17: SEM Image of the Dark Region of the Rock Sample.....26

Figure 18: Spectrum of the Elements from the Dark Region of the Rock Sample. 27

Figure 19: SEM Image of the Light Region of the Rock Sample 28

Figure 20: Spectrum of the Elements of the Light Region of the Rock.....29

Figure 21: Before and After Acid Injection Pictures of Sample F.....32

Figure 22: Before and After Acid Injection Pictures of Sample B.....32

Figure 23: Leak-Off Schedule for Samples A-F.....33

Figure 24: Leak-off Data for Sample A-F (Excluding Sample E).....34

Figure 25: Fracture Conductivity vs. Closure Stress for Samples A-E.....36

Figure 26: Effect of Chelating Agent on Sample D.....38

Figure 27: Fracture Conductivity Comparison of Outcrop and Field Samples.....42

LIST OF TABLES

Page

Table 1: Chemical Composition of the Dark Region of the Rock Sample 27

Table 2: Chemical Composition of the Light Region of the Rock Sample.....29

Table 3: Injection Conditions.....30

Table 4: Qualitative Summary of Acid Interaction.....31

Table 5: Cumulative Leak-Off Volume for Samples A-F.....35

CHAPTER I

INTRODUCTION AND LITERATURE REVIEW

Introduction

Hydraulically fracturing a well in a hydrocarbon reservoir attempts to increase the conductivity of a fracture network and ultimately, the productivity of the well. If the pressure of an injected fluid exceeds the fracture pressure of the formation, the rock cracks and creates an artificial fracture. The creation of artificial fractures allows the intersection of more natural fractures that otherwise do not physically intersect the wellbore. More pore volume of the reservoir rock can be drained to the wellbore if a larger fracture network is created (Mukherjee 1993; Newman et al 2009).

However, the stresses of the formation will cause the fracture that is created to close. Fracture closure is controlled by elastic, plastic, and viscous rock properties. (Abass 2006). A mechanism to ensure a fracture remains open is required. The use of a physical proppant to hold open a fracture is a technique used in many reservoirs. The ultra-low permeability sandstone wells are prime candidate for the use of proppant based hydraulic fracturing. The mechanism addressed in this thesis, however, is acid fracturing. Instead of relying on a physical mechanism to maintain conductivity, acid fracturing relies on the exothermic reaction of hydrochloric acid (HCl) and calcium carbonate ($CaCO_3$) found in the rock (Lund et al. 1974; Newman et al 2006). The reaction produces calcium chloride salt ($CaCl_2$), carbon dioxide gas (CO_2), and water (H_2O). The reaction of HCl and carbonate is

$$CaCO_3(s) + 2\,HCl(l) \rightarrow CaCl_2(s) + CO_2(g) + H_2O(l)$$

The reaction results in carbonate rock dissolving in the presence of acid. If successful, the dissolution of the carbonate rock will create uneven surface in the formation. Under the stresses present in the formation, the fracture is propped open with less dissolved regions acting as pillars and more dissolved regions acting as channels for flow (Economides 2012). Figure 1 illustrates the creation of a fracture, the dissolution of the rock in the presence of acid, and the resulting conductivity upon fracture closure.

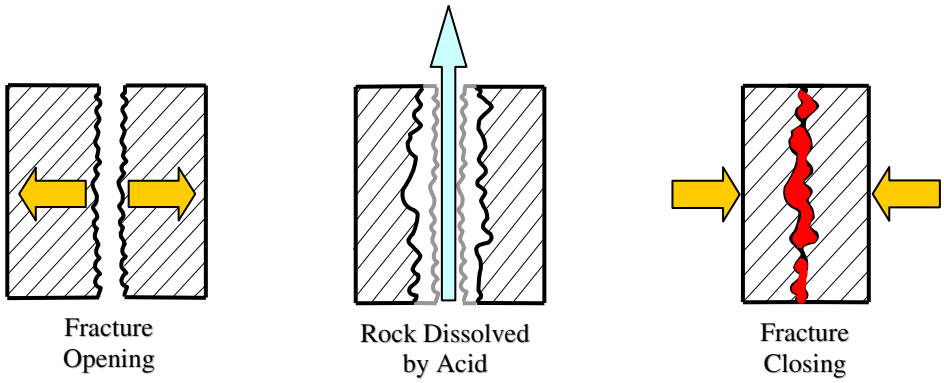

Figure 1: Fracture Formation in the Presence of Acid (After Pounik 2008)

A successful acid fracturing treatment will result in increased production from the stimulated well. The extent to which production is increased is a function of the fracture length and the fracture conductivity. The fracture length is influenced by how far from the wellbore the reactive acid transports along the walls of the fracture, or the acid penetration distance (Williams and Nierode 1972). Although the exact distance is difficult to predict, the fracture length is affected by the acid injection rate, the acid reaction rate, and the acid loss rate (Abass 2006). The industry has developed gelled acids to improve the effectiveness of acid fracture treatments. For some applications,

gelled acid allows greater fracture penetration by increasing fracture width, slowing reaction rate, and reducing fluid loss (Crowe et al 1981).

Literature Review

Acid Fracturing

Hendrickson et al. (1960) studied the effect of flow velocity and fracture width on acid reaction rate. The study focused on varying horizontal-linear fracture widths and injection velocities and the effect on acid penetration. Increasing the injection rate of 15% HCl or the presence of a wider fracture will result in deeper acid penetration before spending. However, Hendrickson et al. also determined that the effect of increasing the injection rate on acid penetration diminishes. Increasing shear rate will increase the reaction rate due to the reaction of HCl and carbonates be first-order diffusion controlled.

Research by Navarrete et al. (1998) focused on the difference in fracture length and fracture conductivity when using neat 28% acid and emulsified 28% acid. The fracture conductivity of limestone samples was studied in a laboratory fracture conductivity apparatus similar to the one used in the research included in this thesis. Acid fracture simulations and a new technique were developed to measure key reaction parameters. Navarrete et al. (1998) concluded that emulsified 28% HCl provides a more efficient use of the acid capacity and allow longer fracture lengths while not sacrificing fracture conductivity.

Further experimental research conducted by Melendez (2007) and Pournik (2008) examined the relationship of rock strength, channel etching, and fracture

conductivity. Melendez studied the effects of hardness and channel formation in three rock types, Texas cream chalk, San Andres Dolomite, and Indiana limestone. Melendez concluded that the presence of channeling in the rock dominates fracture conductivity behavior after closure. However, in the absence of channeling, rock strength dominates fracture conductivity after closure. Pournik tested different acid systems and the characterized the resulting etching patterns and affect on rock-strength. Pournik concluded that an optimal acid system exists for a particular formation type, contact time, and overburden stress. Finally, Pournik developed a correlation to predict fracture conductivity that includes surface etching roughness parameters. The experimental equipment and procedure used by Martinez (2007) and Pournik (2008) is essentially identical to the one used in this thesis.

Fracture Conductivity Correlation

Nierode and Kruk (1973) developed correlations to predict fracture conductivity from producing drawdown, rock embedment strength, and dissolved rock equivalent conductivity. The correlations are based on the assumption that the fracture surface is dissolved uniformly, producing a channel of constant width. The corresponding fracture conductivity associated with the channel is termed the dissolved rock equivalent conductivity (DREC). Additional considerations for the rock strength (RES) and amount of closure stress applied are included in the Nierode and Kruk model. Equations 1, 2, and 3 can be used to calculate fracture conductivity from the Nierode and Kruk correlations.

$$k_f \mathrm{w} = C_1 \exp[-C_2 \bullet \sigma_c] \quad \text{.....(1)}$$

$k_f w$ is fracture conductivity in md-in and σ_c is closures tress in psi.

$$C_1 = 0.265 \bullet [\text{DREC}]^{0.822} \quad \text{.....(2)}$$

$$C_2 \bullet 10^3 = \begin{cases} 19.9 - 1.3 \bullet \ln(\text{RES}) & if\ 0 < \text{RES} < 20{,}000 \text{ psi} \\ 3.8 - 0.28 \bullet \ln(\text{RES}) & if\ 20{,}000 < RES < 500{,}000 \text{ psi} \end{cases} \quad \text{.....(3)}$$

Clay-Swelling

The presence of clay minerals in a formation presents challenges when using fresh water. Certain clay minerals swell when contacted with fresh water and reduce the size of the flow channels in the formation (Black and Hower 1965). Clays consist of negatively charged aluminosilicate layers kept together by cations. The most characteristic property is their ability to adsorb water between the layers, resulting in strong repulsive forces and clay expansion (Hensen and Berend 2002). However, the use of a potassium chloride (KCl) solution controls the swelling of clays. Obrien and Chenevert (1973) provide a detailed explanation of the stabilization of clays in the presence of potassium chloride. In summary, through cation exchange, potassium replaces sodium and calcium and provides the clay a more stable structure that has a resistance to swelling. Furthermore, potassium chloride can be used economically and is compatible with a range of other chemicals used in water fracturing such as friction reducers, fluid-loss additives, and surfactants (Black and Hower 1965). The samples used in this study had significant clay-like content. To prevent swelling, a 2% KCl solution was used throughout the experiment.

Research Objectives

The main objective in the research presented in this thesis is to determine the effectiveness of 15% HCl as an agent of well stimulation for certain carbonate reservoirs. Using experimental parameters representing field conditions, acid injection and fracture conductivity measurements were performed on 6 rock samples to achieve the following objectives:

- Use images of each sample taken before and after acid injection to determine the extent to which 15% HCl reacted with the sample by qualifying the amount of rock volume dissolved.
- Measure fracture conductivity at increasing values of closure stress to determine if higher acid solubility of each sample corresponds to higher fracture conductivity.
- Observe the change in fracture conductivity when a rock sample is exposed to a chelating agent.
- Present a final recommendation based on the results of the research presented in this thesis as to whether acid fracturing should be pursued by in the formation as a well stimulation strategy.
- Observe the difference between using outcrop rock samples (i.e. Indiana Limestone or San Andres Dolomite) and field rock samples.

CHAPTER II

SET-UP AND PROCEDURE

Experimental Set-Up

The experimental set-up consists an acid injection apparatus, a fracture conductivity measurement apparatus, and a profilometer. The details of each system are discussed below.

Acid Injection Apparatus

The acid injection and fracture conductivity measurement uses a modified API conductivity cell that holds the samples in place during the experiments. The cell is corrosion resistant and can withstand pressures that greatly exceed experimental conditions. Figure 2 shows the conductivity cell and accompanying side pistons.

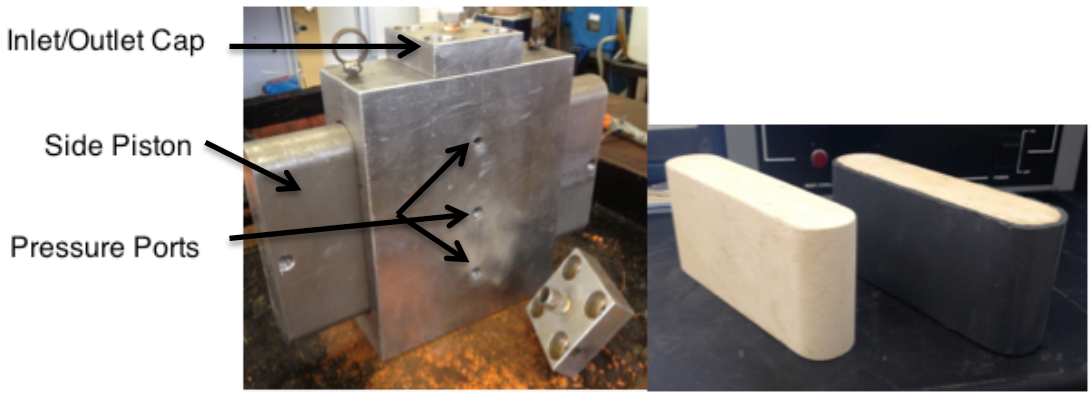

Figure 2: Modified API Cell and Rock Samples

The dimension of the cell are 10” x 3 1⁄4” x 8”. The interior of the cell contains a 7 1⁄4” x 1 3⁄4” space for the rock samples (Malagon 2006). Two internal O-rings are super-glued into slots in the cell to provide a seal around the rock samples. The top and

bottom of the cell contain a flow line for fluids to flow into and out of the cell. The connections for the flow lines are ½ inch Swagelok fittings. Three pressure ports in the middle of the cell provide pressure readings of the cell and across the fracture. Two pistons accompany the cell and are inserted into the open slots once the rock samples are in place. The side pistons contain O-rings to prevent fluids from escaping from the cell during acid injection and fracture conductivity measuring. The side pistons also contain a pressure port to measure leak-off pressure and volume during acid injection.

The acid injection system is designed to flow acid through the API cell at high pressures (greater than 1000 psi). The pressure transducers display the pressure inside the cell, across the fracture, and the leak-off pressure (across the samples). The Chem-Pump is a metered pump that is able to flow up to a rate of 1.05 liters/minutes. One liter per minute scales to 20 barrels per minute under field conditions (Pournik 2008). Acid is injected from the bottom of the cell to the top to avoid gravitational effects. Spent acid is properly disposed of in large chemical drums. Thermocouples located upstream and downstream of the cell provide temperature data during the injection. Finally, backpressure regulators ensure that the system stays at the desired pressure of 1000 psi. CO_2 is produced from the reaction of HCl and $CaCO_3$. Keeping the system at a pressure greater than 1000 psi ensures that the CO_2 produced remains in solution. The acid injection apparatus is shown in Figure 3.

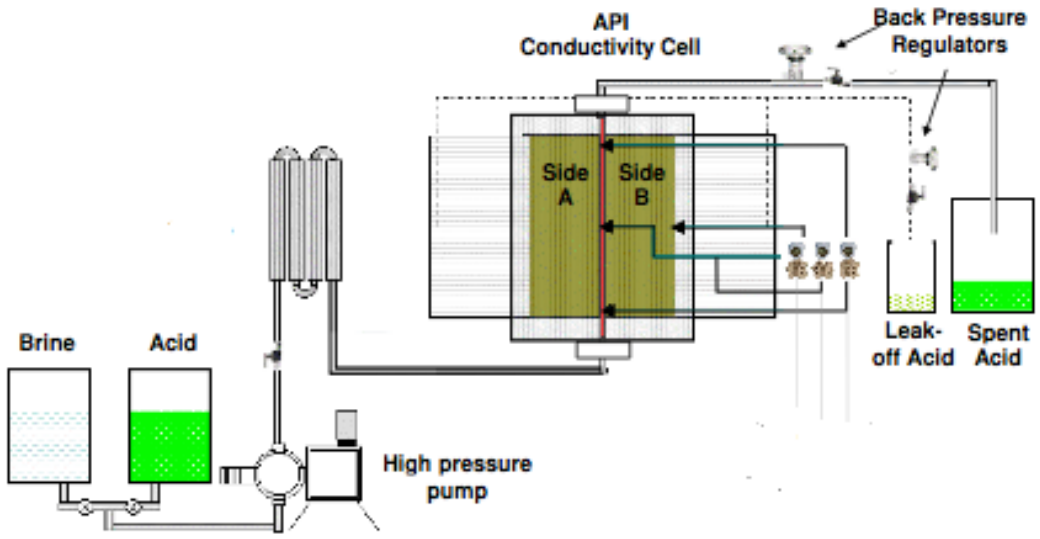

Figure 3: Schematic of Acid Injection Apparatus (After Zou 2005)

Fracture Conductivity Measurement Apparatus

The apparatus used to measure fracture conductivity is designed to flow a fluid through the API cell that is subject to varying closure stresses. A load frame holds the cell in a horizontal position. Pressure transducers measure the pressure across the fracture and in the cell. Three pressure transducers measure different ranges of pressure drop. Depending on the pressure measurement requirements, pressure drops in the 0 to ten psi, 0 to 30 psi, and 0 to 100-psi ranges can be measured. A thermocouple located downstream of the cell provides temperature data. The load frame contains a piston that can apply force to the cell. Increasing this force applies closure stress to the samples inside of the cell. Figure 4 shows a schematic of the apparatus used to measure fracture conductivity.

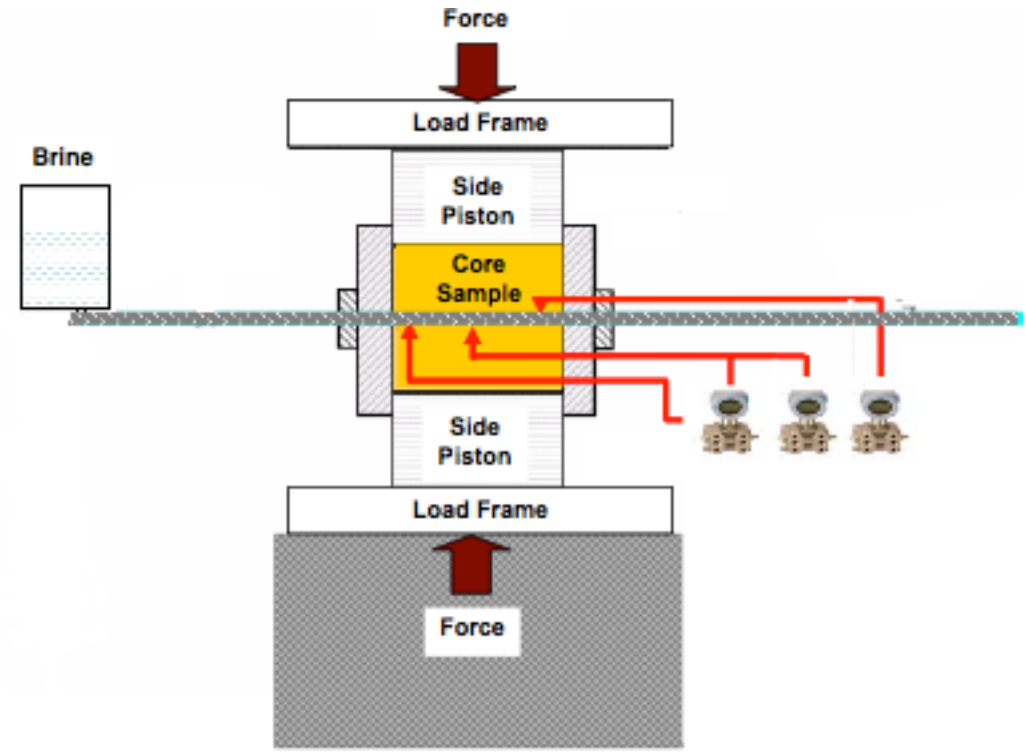

Figure 4: Schematic of Conductivity Measurement Apparatus (After Zou 2005)

The flowrate of the fluid flowing through the cell is measured using a stopwatch and a graduated cylinder. At each closure stress, pressure across the fracture, flowrate, and fluid viscosity is recorded. The fracture conductivity is calculated using Darcy's flow equation.

Profilometer Apparatus

The surface of the rock samples can be scanned with a profilometer before and after acid injection to determine the volume of rock removed during the acid injection. Figure 5 shows the profilometer set-up.

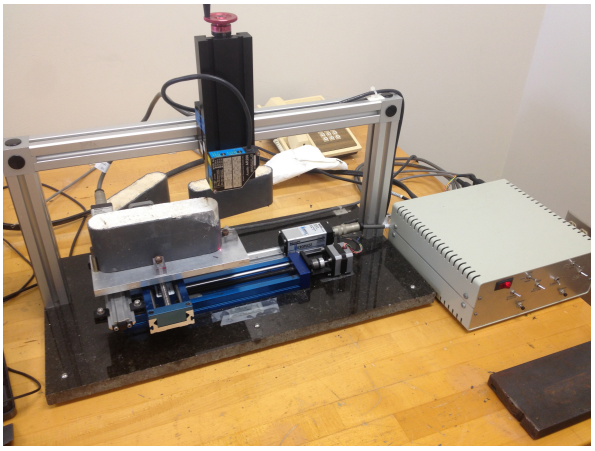

Figure 5: Profilometer Used to Determine Volume Removed

The apparatus includes a laser sensor, control box, and PC software interface. The profilometer uses the laser displacement sensor to record the vertical height of the sample as it travels over the entire length and width of the sample. Figure 6 shows the path that the profilometer takes to scan each core.

Figure 6: Path of Profilometer Scan (After Melendez 2007)

Matlab is used to compare the scan before and after the acid injection to generate the volume removed as well as an illustration of the etched region of the sample. Ultimately, the volume of rock removed can be used in acid fracture conductivity

correlations, such as the one presented by Nierode and Kruk, to predict the fracture conductivity. However, due to the brittle nature of the rock samples in this experiment, removing the rock samples from the cell and scanning between the acid injection and conductivity measurements was not feasible. Therefore, the volume removed during acid injection was not determined for this experiment.

Experimental Procedure

The experimental procedure can be split into 4 tasks: rock sample preparation, cell preparation and loading, acid injection, and fracture conductivity measurement. Figure 7 shows the progression of the procedure through the three tasks.

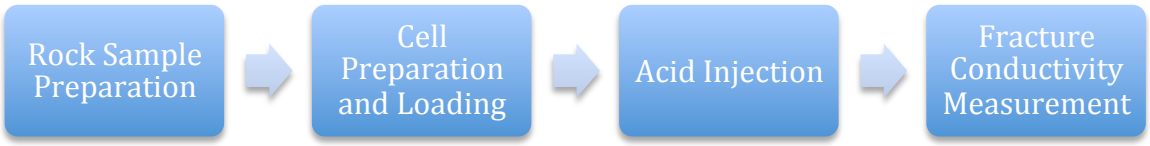

Figure 7: Experimental Procedure Flowchart

Rock Sample Preparation

The field rock samples are delivered from Kocurek Industries where they are sawed, not fractured, into two pieces for acid inject. Rock sample preparation begins with using an adhesive to secure the rock sample to a composite piece of rock. The samples submitted for acid injection are less than 3.5 inches thick. The samples must be glued to a complementary piece of rock to be the required thickness for acid injection. The rock samples are covered with a layer of silicone before being loaded into the cell.

The silicone is applied with a mold that will give the rock samples a shape identical to the cell.

- Apply a thin layer of Gorilla Glue™ to the surface of the composite rock.
- Place the rock sample firmly placed on top and use C-clamps to apply force perpendicular to the interface of the rock samples. The force applied by the C-clamps ensures that the two pieces firmly adhere.
- Clean excess glue that is forced out from between the rock samples with a paper towel.
- Allow the rock samples to stand for 45 minutes while the glue dries.
- Scrape excess glue with a putty knife. Once the Gorilla Glue™ dries, a layer of dried and expanded glue usually forms at the interface of the rock samples. The rock samples are now 3.5 inches thick, the required thickness for acid injection.
- Apply blue painters tape to the top and bottom surfaces of the rock sample.
- Trace the edge of the samples with a razor blade and cut away the excess tape. The tape will prevent the sample surfaces from contamination during the remainder of the Sample preparation. Figure 8 shows the removal of excess tape from the rock sample.

Figure 8: Example of Removing Excess Tape from Rock Sample

- Begin the process of forming the silicone mold by applying a layer of spray paint to the sides of the rock samples. The dusty/brittle nature of the rock samples makes it difficult for silicone to adhere to the rock sample. The spray paint provides a contact for the silicone to bond with.
- Place the samples under a fume hood and allow the spray paint to dry for 45 minutes.
- Apply a layer of silicone primer (SS4155) evenly to the rock samples using a foam brush. Allow the samples to dry for 15 minutes after the primer is applied. Figure 9 shows the first application of silicone primer using the sponge brush to the rock sample.

Figure 9: Application of Silicone Primer

- Apply a second layer of primer to the rock samples. Prepare the metal molds that will contain the cell while the silicone primer is drying for 15 minutes.
- Wash the molds thoroughly with acetone and paper towels to eliminate any dried silicone from previous sample preparations.
- Apply Molbydate release spray to the cleaned molds.
- Dry the molds for 2 minutes before a second coat of release spray is applied.
- Assemble the pieces of the metal mold.
- Apply a third and final coat of silicone primer to the rock samples and allow to dry for 15 minutes.
- Prepare the silicone mixture while the primer is drying for the third time. The silicone solution is a 2-part mixture of Silicone Compound and Curing Agent mixed in a 1:1 ratio by mass.
- Stir the Silicone Compound before pouring.
- Add 70 grams of Silicone Compound to a beaker using the mass balance.
- Stir the Curing Agent and add 70 grams to the beaker.

- Mix the silicone mixture thoroughly using a stirrer.
- Place each sample into a mold once the final coat of silicone primer has dried. The rock samples should be centered in the mold to create an even coat of silicone around each sample.
- Pour silicone slowly around each sample at each end. Poring at the middle of each sample can lead to bubbles forming when the silicone hardens. Figure 10 shows the correct way to pour the silicone into the mold. The silicone takes approximately 15 minutes to fill the space between the mold and the rock sample.

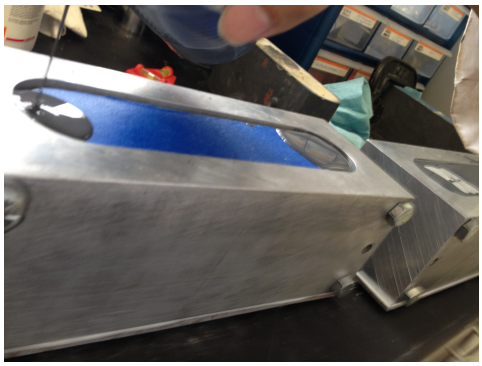

Figure 10: Pouring Silicone at the Ends of the Rock Sample

- Apply plumbers putty to prevent silicone from leaking between the pieces of the mold.
- Allow the molds containing the rock samples to sit for approximately 6 hours. Set the oven at 100^{o} F (3-4 on the 10-scale dial).
- Place the molds in the oven for approximately 2.5 hours.
- Remove the molds from the oven and allow sufficient time to cool.

- Disassemble the metal molds and remove the silicone-covered rock samples
- Photograph the rock samples and saturate in a 2% KCl solution under vacuum for 4 to 6 hours. Figure 11 shows the vacuum pump set-up.

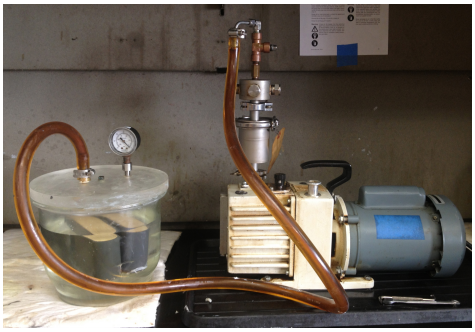

Figure 11: Vacuum Pump Equipment

Cell Preparation and Loading

- Once dry on the surface, wrap the prepared rock samples with a layer of Teflon tape in three areas. The Teflon tape serves as a barrier to prevent acid leaking around the rock samples during acid injection. Figure 12 shows the placement of the three bands of Teflon tape on the rock sample.

Figure 12: Placement of Teflon Tape on Rock Sample

- Apply vacuum grease (Dow Corn High Vacuum Grease) to the rock samples as well to serve a friction-reducing element. When the rock samples are loaded into the cell, friction can cause the silicone mold to break from the rock sample.
- Prepare the cell for loading and superglue the cell O-rings (251-VT90) that sit inside the cell into position. Stretching the O-rings before applying superglue will insure that the O-rings will fit sufficiently in the cell. Figure 13 shows the cell before and after the O-ring is inserted into the proper groove.

Figure 13: Placement of O-Rings Inside the Cell

- Place the cell in the loading frame.
- Load the rock samples into each side of the cell with a hydraulic hand pump.
- Use the metal shin to ensure a 0.12 inch space remains between the faces of each rock sample. The space replicates the fracture width in a formation.
- Secure the pistons' O-rings (351-VT90) and load the pistons likewise into the cell.
- Place the cap O-rings (123-VT90) on the caps.
- Apply O-ring grease (Dow Corn 55) to the caps' O-rings.

- Attach the top and bottom caps of the cell to fully enclose the rock samples into the cell.
- Match the ports on the cell with the appropriate 1/8 in tubing lines that are connected to pressure transducers.
- Attach the ½ inch inlet and outlet hoses to the top and bottom caps of the cell. The cell is prepared and ready for acid injection.

Figure 14 shows the cell once all pressure and flow lines have been correctly installed. A heating jacket is placed around the cell to provide additional heat during the injection.

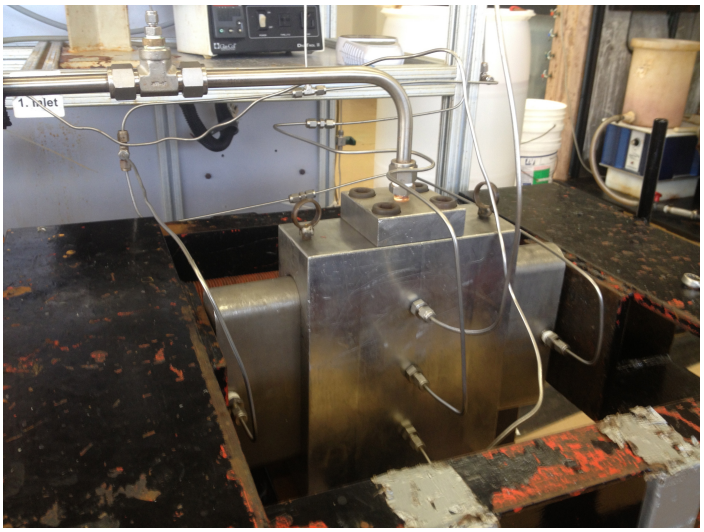

Figure 14: Cell Prepared for Acid Injection

Acid Injection

The appropriate personal protective equipment for preparing and injecting the acid includes latex gloves, a lab-coat, and a full-face respirator. The procedure to prepare and inject acid is detailed below.

- Prepare the 2% KCL solution. The injection conditions required a temperature of 140^{o} F. The heating element of the acid injection apparatus is unable to heat the 2% KCl solution to the required temperature. For additional heating, two submersible heaters pre-heated the KCl solution. The KCl solution cycles through the cell until the injection fluid reaches 135^{o} F.
- Prepare the 15% HCl while the injection fluid reaches the required temperature. Per the injection conditions, 18 liters of 15% by weight HCl solution is required.
- Mix HCl with water under the fume hood to create the 15% HCl solution.
- Stir the 15% HCl with the paddle mixer while waiting to be injected.
- Once the acid is prepared and the KCl solution has reached 135^{o} F, pressurize the cell to 1000 psi.
- Using the back-pressure regulator, maintain a 20-psi leak off pressure drop throughout the injection.
- Perform a final check for leaks through the pipe-fittings and the cell ports.
- To begin injection, close the 2% KCl solution inlet valve and open the acid inlet valve so that the acid solution is pumped through the system.
- At 1-minute intervals, record the temperature upstream and downstream of the cell as well as the leak-off volume.
- After 15 minutes, close the acid inlet valve and open the 2% KCl solution valve to flush the system.
- Once the system is sufficiently flushed and drained, remove the 1/8 inch tubing from each port on the cell, as well as the inlet the ½ inch inlet and outlet hoses.

- Hoist the cell, pistons and end caps included, from the injection frame using a hydraulic hand pump.
- Place the cell on the transfer cart and move the cell to the fracture conductivity measurement apparatus.

Fracture Conductivity Measurement

- Load the cell into the fracture conductivity measurement frame.
- Attach the ½ inch inlet and outlet hoses to the caps of the cell. The flow should enter through the opposite cap used for the inlet during acid injection. The flow is now horizontal.
- Attach the appropriate 1/8 inch tubing to the correct pressure ports to measure the cell pressure and pressure drop across the fracture.
- Activate the hydrostatic pump to close the load frame piston. Although the hydrostatic pump does not apply closure stress to the cell at this time, the cell is held in place by the load frame piston for the initial fracture conductivity measurements. Figure 15 shows the cell correctly prepared for fracture conductivity measurement.

Figure 15: Cell Prepared for Fracture Conductivity Measurement

- Circulate the 2%KCl solution through the fracture conductivity measurement apparatus.
- Record the first fracture conductivity measurement 4 to 6 hours after circulation begins. The delay allows the system to reach equilibrium.
- For the first fracture conductivity measurement, record the pressure drop across the cell.
- Calculate and record the flowrate using a stopwatch and graduated cylinder. Measure the flowrate three times and calculate the average flowrate.
- Record the temperature and the corresponding value for the viscosity of water.
- Calculate the fracture conductivity using.
- Repeat the calculation of fracture conductivity every 30 minutes until the fracture conductivity reaches a constant value. When the fracture conductivity at zero closure stress is determined, the hydrostatic pump is activated to apply closure stress

to the cell in 500-psi increments. The procedure to determine the fracture conductivity of the rock sample is repeated under the new closure stress condition. The fracture conductivity is calculated for each change in closure stress until the either the rock breaks or the flowrate is not great enough to be accurately measured.

The cell can be removed from the loading frame once the final fracture conductivity calculation is recorded for the highest obtainable closure stress condition. The hydraulic hand pump lifts the cell from the loading frame and the cell is placed on a cart. The cell is lowered to the injection apparatus for disassembly. The pistons, end caps, and the rock samples are removed. The rock samples are photographed and excess O-ring grease and Teflon tape is removed. The cell is cleaned with acetone and paper towels to remove superglue, O-ring pieces, and any remaining silicone.

Conductivity Calculations

The calculation of fracture conductivity is derived from Darcy's law describing the flow of fluids through a porous media.

$$\boldsymbol{Q = \frac{k \bullet A}{\mu}\frac{(\Delta P)}{L}} \quad \text{.....(4)}$$

Where Q is the flowrate in $\frac{\text{cm}^3}{\text{s}}$, k is the permeability in darcies, A is the cross sectional area of flow in cm^2, μ is the viscosity in cP, ΔP is the pressure drop across the porous material in psi, and L is the thickness of the porous material in cm.

The calculation of fracture conductivity solves for the permeability of the fracture from Equation 4 and multiplies the permeability with the fracture width. Equation 4 is separated into fracture height and fracture width. The fracture height of

the samples used in this research is 1.61 inches. The fracture height includes the thickness of silicone on each side of the rock samples (0.045 inches). The thickness of the samples is equal to the distance between the two pressure ports of the cell. The distance is equal to 5.375 inches. Flowrate, pressure drop, and viscosity are determined experimentally during the fracture conductivity measurements. To account for the changes in units from SI to field units, a coefficient of 8030 is included in the calculation. Solving for fracture conductivity, k_fw, Equation 4 becomes:

$$k_f w = \frac{8030 \cdot Q \cdot \mu \cdot L}{\Delta P \cdot h} \quad \text{.....(5)}$$

Where k_fw is the fracture conductivity in md-ft, Q is the flowrate in $\frac{\text{L}}{\text{min}}$, L is equal to 5.375 inches, and h is equal to 1.61 inches.

CHAPTER III

EXPERIMENTAL RESULTS AND DISCUSSION

Six core samples were tested in this study to evaluate the feasibility of acid fracturing stimulation. The six samples, labeled A-F in order of increasing acid solubility, were removed from different depths of a carbonate formation. The samples varied in color and, most notably, exhibited varying acid solubility.

SEM-EDX Analysis

SEM-EDX analysis of a rock sample from the formation was conducted. Powder from the rock samples was scraped from the surface and analyzed using a scanning electron microscope and element identification system (EDX). Figure 16 shows a cross-sectional view and side view of the rock sample used for the SEM-EDX analysis.

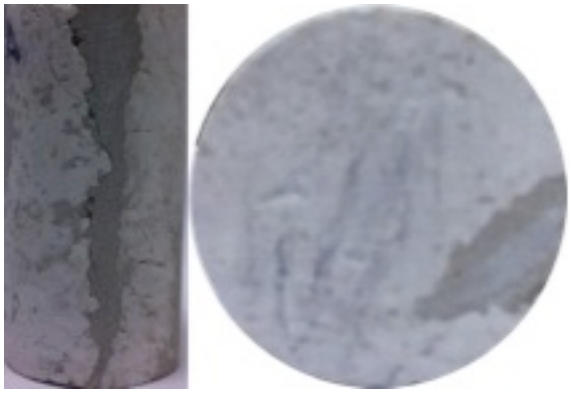

Figure 16: Rock Sample for SEM/EDX Analysis

Figure 16 shows that the rock sample is made up of a dark region and a light region. SEM-EDX analysis of powder removed from the surface of the two regions indicates the chemical makeup of the rock. Figure 17 contains the image of the dark region taken from a scanning electron microscope (SEM).

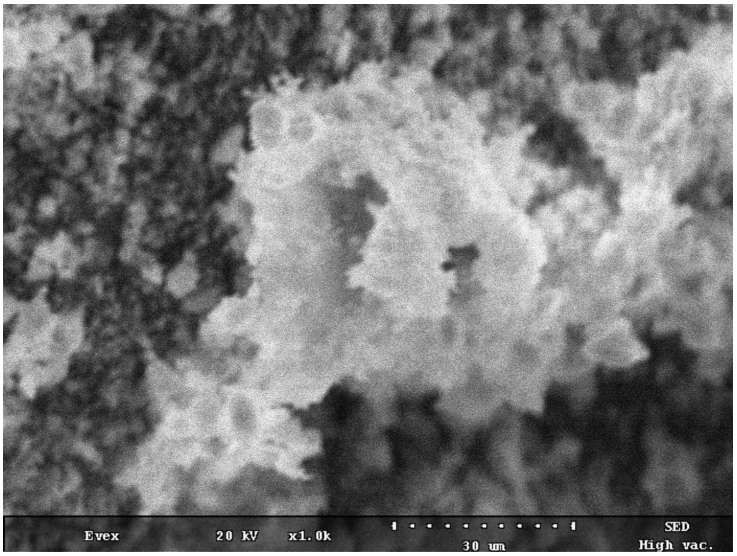

Figure 17: SEM Image of the Dark Region of the Rock Sample

Figure 18 shows the EDX results of the dark region of the rock sample.

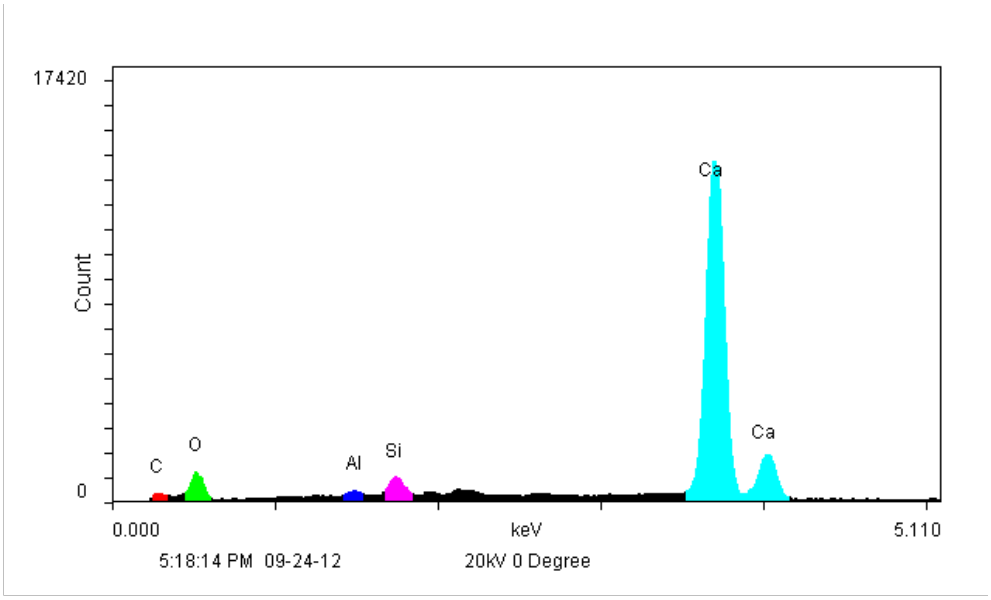

Figure 18: Spectrum of the Elements from the Dark Region of the Rock Sample.

From Figure 18, the dark region of the rock sample has significantly more Ca^{2+} ions. The presence of elevated amount of Ca^{2+} indicates that this region is mostly carbonates, $CaCO_3$.

Table 1 includes the weight percentage of each positive ion.

Table 1: Chemical Composition of the Dark Region of the Rock Sample

Element	Weight %
C	13.76
O	52.56
Al	0.43
Si	1.66
Ca	31.59

The results of the SEM-EDX analysis suggest that the dark region of the rock sample is predominantly carbonate. As mentioned, the use of HCl acid is most effective with carbonate materials.

Figure 19 contains the image of the light region taken from a scanning electron microscope.

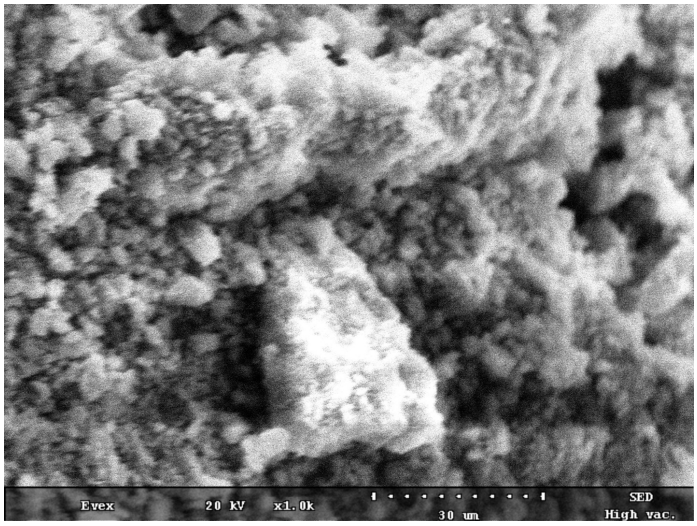

Figure 19: SEM Image of the Light Region of the Rock Sample

Figure 20 shows the EDX results of the light region of the rock sample.

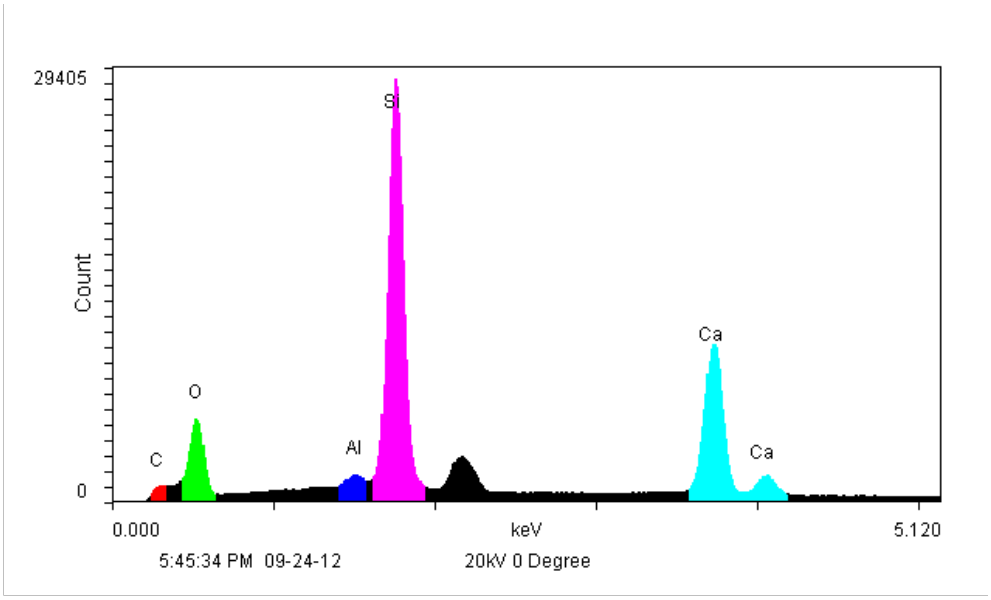

Figure 20: Spectrum of the Elements of the Light Region of the Rock

From Figure 20, the light region of the rock sample has significantly more Si^+ and Al^+ ions. The presence of elevated amount of Si^+ and Al^+ ions indicates that this region is mostly aluminosilicate, which is a major component of clay.

Table 2 includes the weight percentage of each positive ion.

Table 2: Chemical Composition of the Light Region of the Rock Sample

Element	Weight %
C	17.63
O	52
Al	1.15
Si	20.36
Ca	8.86

Unless stabilized, the interaction of HCl and clays can cause plugging as the H^+ ions replace the Al^+ ions in the clay matrix. The Al^+ ions are leached away and form a layer that impedes flow. The use of hydrofluoric acid is an effective means to dissolved aluminosilicates (Gdanski 2000).

Acid Injection

The following experimental conditions were specified to closely mimic field treatment conditions. The acid injection temperature was 135º F. The acid system was 15% HCl by weight in a 2% KCl solution. The 2% KCl brine acted to control clay swelling in the presence of water. No additional additives were included in the acid system. The acid injection rate was 1 liter per minute. The acid contact time was 15 minutes. The acid injection conditions are included in Table 3.

Table 3: Injection Conditions

Injection Rate	1 Liter/minute
Injection Duration	15 minutes
Temperature	135º Fahrenheit
Leak-Off Pressure	20 psi
Additives	2% KCl
Acid System	15% HCl

During each acid injection periods, acid leak-off data and temperature data upstream and downstream of the cell are collected. The pictures of each sample before

and after the acid injection and fracture conductivity measurements are included in Appendix A. The pictures provide qualitative data in regards to the extent of acid interaction with Samples A-F.

Table 4 provides a summary of the qualitative observations made from the acid interaction with each sample.

Table 4: Qualitative Summary of Acid Interaction

	Acid Solubility	Surface Observations
Sample A	2.67%	No observable surface change
Sample B	6.87%	No observable surface change
Sample C	18.13%	No observable surface change
Sample D	44.44%	Limited surface change
Sample E	51.05%	Noticeable surface change, dissolution of dark, carbonate regions
Sample F	73.22%	Significant surface change, significant dissolution of dark carbonate regions

From

Table 4, Samples E and F, which have a greater acid solubility, showed a greater amount of surface alteration after acid injection. Figure 21 shows the surface of Sample F before and after acid injection.

Figure 21: Before and After Acid Injection Pictures of Sample F

Samples A, B, and C, which have a lower acid solubility, showed very little surface change after acid injection. Any surface alterations appeared to be more related to the stress of the fracture conductivity measurements or unloading of the samples from the cell. Figure 22 shows the surface of Sample B before and after acid injection.

Figure 22: Before and After Acid Injection Pictures of Sample B

Sample D, with moderate acid solubility, showed marginal surface change. The dark regions of Samples E and F, which have been identified as predominately carbonate regions, showed the most dissolution. In particular, Sample F showed significant dissolution in the carbonate regions of the sample. Samples D, E, and F also showed signs of some worm-holing.

The results of the acid injection of Samples A-F include leak-off data collected during the injection. As mentioned, the leak-off pressure was set at 20 psi for each acid injection. Figure 23 shows the leak-off schedule for each sample over the 15-minute acid injection.

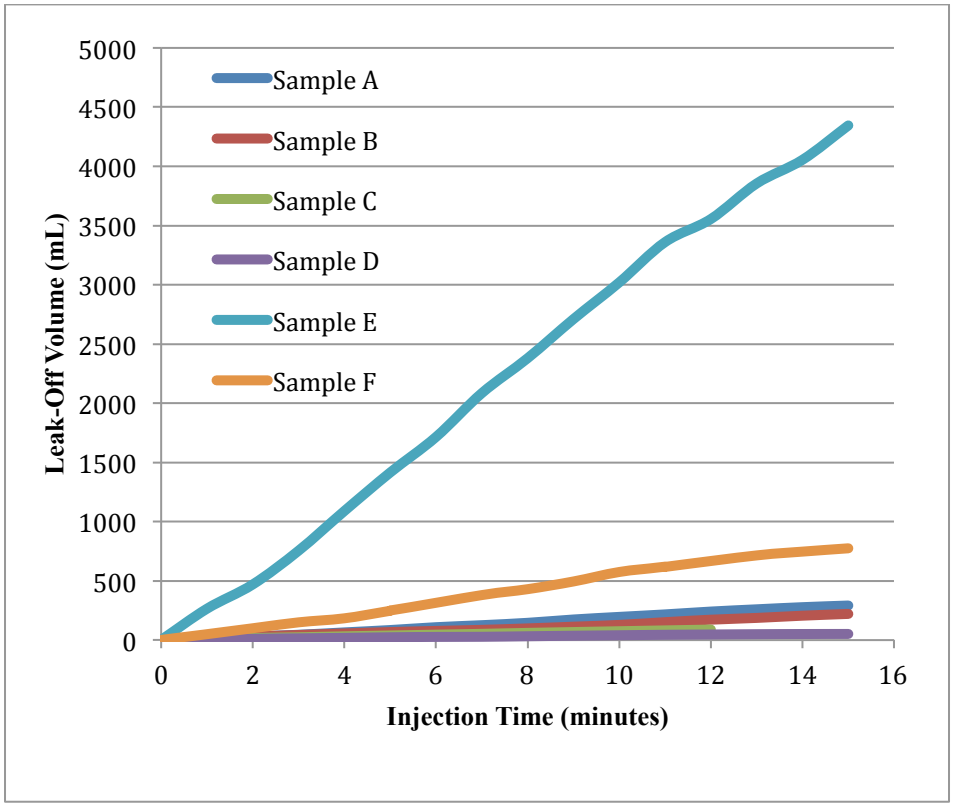

Figure 23: Leak-Off Schedule for Samples A-F

Figure 24 shows the same leak-off schedule with Sample E removed to distinguish between the other samples' data.

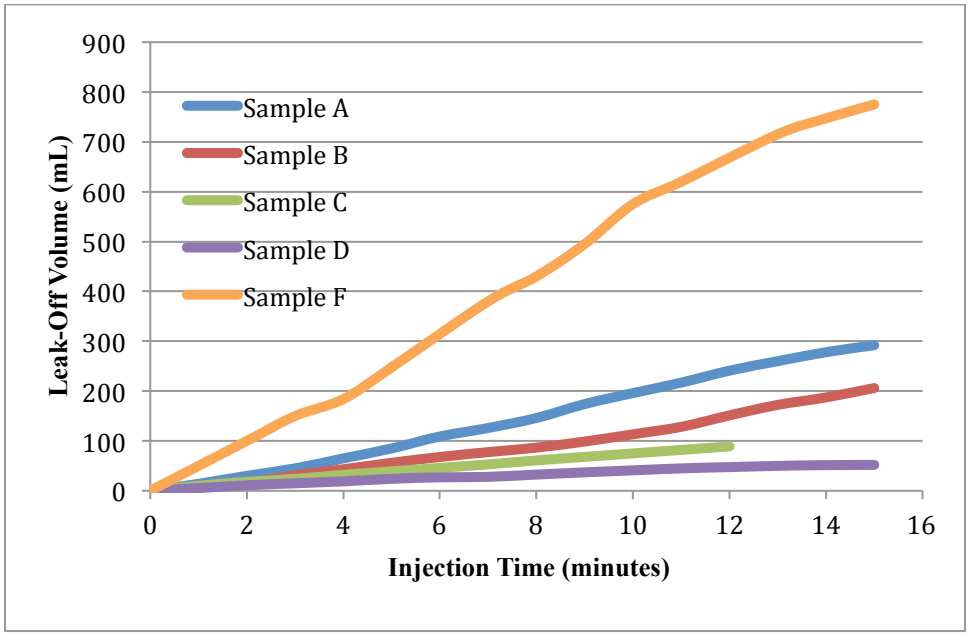

Figure 24: Leak-off Data for Sample A-F (Excluding Sample E)

From Figure 23 and Figure 24, the leak-off is observed to increase linearly over the course of acid injection. The leak-off schedule can be used to identify if the acid forms a wormhole. A wormhole is a channel that forms in a direction perpendicular to the flow. Once a wormhole breaks through the rock sample, a sudden increase in leak-off volume would be expected. Such an increase is not identified in the six samples presented. Sample E demonstrated the highest leak-off rate over the course of acid injection. Over the 15-minute injection period, approximately 4.5 liters of acid traveled through the sample. Sample F demonstrated the second most amount of leak-off. Samples C and D showed the least amount of leak-off, both less than 100 milliliters. Table 5 shows the cumulative leak-off volumes for each sample.

Table 5: Cumulative Leak-Off Volume for Samples A-F

Sample	Cumulative Leak-Off Volume (mL)
A	292
B	221.1
C	89*
D	52
E	4345
F	775

The cumulative leak-off volume for Sample C cannot be directly compared to the leak-off values of remaining samples. During the injection, the O-ring between the cell and one piston failed. The increased pressure in the cell caused the piston to shift and fluid leaked from the system. As a result, the injection was stopped and only 12 minutes of data was collected. It is assumed that had the experiment continued uninterrupted, the cumulative leak-off volume would be greater than the 89 mL collected.

Fracture Conductivity

The fracture conductivity measurements were performed by flowing 2% KCl solution through the API cell. The fracture conductivity was calculated from the pressure across the sample, the brine flowrate, and the experimental properties for increasing amounts of closure stress applied to the samples. The results of the fracture conductivity measurements for Samples A-E are included in Figure 25.

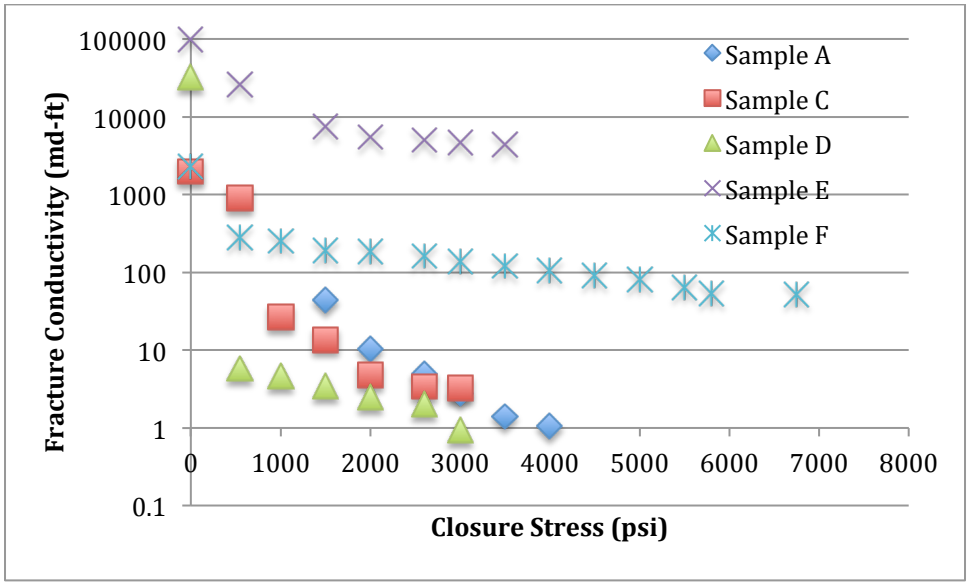

Figure 25: Fracture Conductivity vs. Closure Stress for Samples A-E

Figure 25 shows that for each sample, the fracture conductivity decreases with increasing closure stress. It is important to note that Sample B is not included in Figure 25. During the fracture conductivity measurements, the flow-rate of the brine solution through the cell did not change with increasing closure stress. Inspection of the cell revealed that the brine solution was flowing around Sample B rather than between the samples. Unwanted space between the silicone-covered sample and the cell results in the brine solution flowing around the samples and compromises the results of fracture conductivity measurements. From Figure 25, Samples E and F have the highest fracture conductivity. This could be a result of greater interaction between the acid and Samples E and F, as suggested by the analysis of the samples' surfaces before and after acid injection. However based on this theory, Sample F would be expected to have a higher fracture conductivity than Sample E. While Sample F has a higher acid solubility than

Sample E, the heterogeneity of both samples will play an important role in what areas of the fracture surface are characterized by higher acid solubility. As shown in the photographs of Sample E and F found in Appendix A, darker carbonate regions of Sample F ran perpendicular to the fracture. Therefore, if acid dissolved these local regions of Sample F rather than uniformly dissolving along the length of the fracture, as seen in Sample E, the resulting fracture conductivity would be lower in Sample F. Sample A yielded the next highest fracture conductivity but displayed little sign of acid interaction. While perhaps being a function of acid interaction, the resulting fracture conductivity in each sample may be better explained by the inherent matrix permeability of the rock samples themselves. From Figure 25 and Table 5, the fracture conductivity correlates with the cumulative leak-off volume for each sample. If a rock sample has inherently higher matrix permeability, i.e. Sample E, the fluid used for the fracture conductivity measurement will travel through the rock matrix in addition to the fracture.

Effects of Chelating Agent

In addition to the injection of 15% HCl, an additional study was performed on Sample D. The effect of a chelating agent on Sample D was studied by injecting a chelating agent into the sample. The acid injection apparatus was used for the chelating agent study. However, instead of flowing the chelating agent through the system at a particular rate and contact time, the chelating agent was shut in the cell for four hours. A valve downstream of the cell was closed and the chelating agent was pumped into the system. The pressure of the cell was set to 1000 psi with a leak-off pressure of 5 psi. Every hour, additional chelating agent was added to the system to replace the amount

lost to leak-off. Fracture conductivity measurements were repeated for Sample D and the results of the measurements before and after injecting the chelating agent are shown in Figure 26.

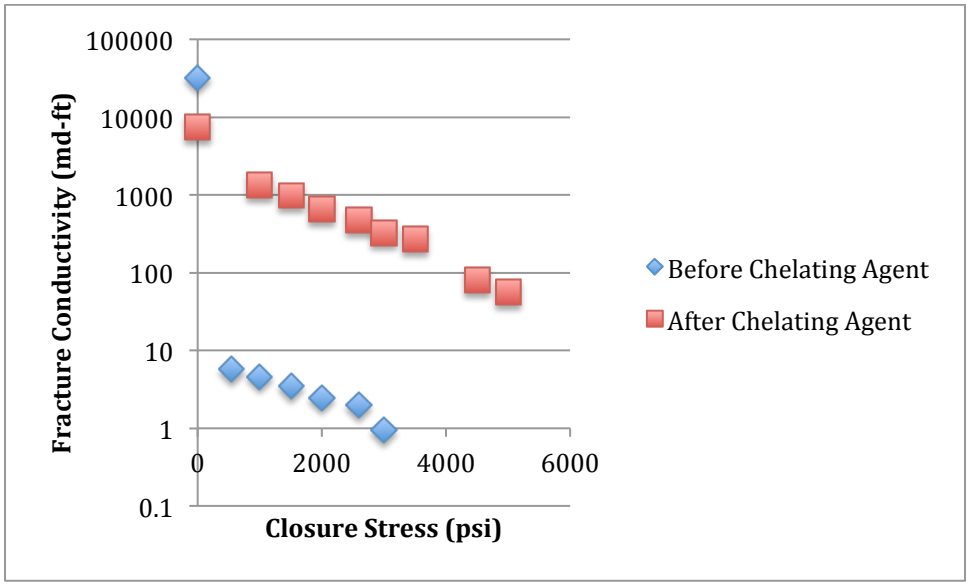

Figure 26: Effect of Chelating Agent on Sample D

Figure 26 shows that the fracture conductivity greatly increased after injecting the chelating agent. Using four hours instead of 15 minutes for contact time likely plays a significant role in increasing the rock dissolution, which could result in increasing fracture conductivity. Based on the increase in fracture conductivity, additional study of the use of chelating agent should be performed.

Comparison of Field Samples and Outcrop Samples

Using rock samples from the field presents challenges not associated with acid fracturing research on outcrop samples. Two outcrop rock samples, Indiana Limestone and San Andres Dolomite, are used to study acid fracturing in the laboratory. Research with outcrop samples have provided detailed models that predict the behavior of these rocks when used for acid fracturing. The outcrop samples chosen for acid fracturing research are homogenous and are void of any material in the pore spaces. As a result, samples can generally be compared across experiments because the rocks are all assumed to share the same properties. This assumption is not valid when working with field rock samples. The research included in this thesis offers insight into working with field samples.

Indiana Limestone and San Andres Dolomite outcrop rocks are convenient to study in the laboratory because the rock can be cut into the correct size and shape for the API cell. Whether cut to form a smooth surface or fracture surface, Indiana Limestone and San Andres Dolomite retains its strength and does not chip during the cell preparation and loading portion of the set-up. By using rock samples that are strong enough to withstand the cutting and shaping process, the results of fracture conductivity analysis describe the behavior of more robust rock samples. These rock samples may be outliers to typical rock that are not strong enough to be used.

The field samples used in this experiment did not show the same characteristics. Much of the rock that is supplied from the field is lost in trying to create even a single sample for acid injection. The field samples used in this thesis were very brittle and the

smooth fracture surfaces were often chipped as the samples were prepared. Removing the samples between acid injection and fracture conductivity measurement to scan the fracture surface was not performed for fear of breaking the samples. When using field rock samples, it is recommended that future research use more than six samples to account for some of the samples breaking during the procedure.

The samples were also very chalky and required black paint to form a consolidated surface that the silicone would adhere to. Even with paint, the process of preparing the silicone around the samples was repeated for each sample before acid could be injected. Additional attempts to prepare the samples often resulted in additional modification to the fracture surfaces. Samples used in a separate research study did not show the same rock integrity as outcrop samples. During the process of preparing the samples, one sample split into two pieces due to the presence of a natural fracture. This sample was repaired using a resin that would not react to the acid, but allow acid injection to be studied on the remainder of the fracture surface. Another rock sample from the second research study split in two halves during the acid injection, rendering it useless for fracture conductivity measurement. The samples in this study were not strong enough to withstand closure stress and accurate fracture conductivity measurements were unable to be collected. Upon applying 500 psi of closure stress, the samples showed negligible flow when the maximum pressure the apparatus could supply was applied. Additional research should be directed at finding a more effective way to coat field samples.

The Indiana Limestone and San Andres Dolomite outcrop samples are void of any material in the pore spaces of the rock. Before the acid injection, the vacuum pump saturates the rock samples with water, causing the pore spaces to be filled. However, rock samples collected from the field do not necessarily have empty pore spaces. Samples used in a separate research study were saturated with hydrocarbons from the reservoir. The presence of hydrocarbons in the pore spaces made it difficult for the silicone to adhere to during cell preparation. Paint was used to create a layer to which the silicone could attach. Additional study could study the effect of pore spaces filled with hydrocarbons on acid interaction.

As stated, the value of using Indiana Limestone or San Andres Dolomite outcrop samples is that the rock is homogenous. Acid interaction with the rock will be consistent over the fracture surface. Field samples do not typically display this homogeneity. The samples used in the research presented in this thesis contained carbonate regions and aluminosilicate regions. Thus acid reacted to varying degrees along the face of the fracture and will affect wormholing behavior through the field rock sample. The homogeneity of the outcrop rock samples also implies a consistent permeability and porosity. When performing research on outcrop samples, the permeability and porosity are treated as a known variable. These values are typically given by Kocurek Industries, which supplies the outcrop rock samples. The permeability of the field samples is determined in matrix acidizing analysis. Results of this analysis on core samples from the same rock used in acid injection indicate that the rock permeability ranged from 0.66 md to 5.85 md.

The heterogeneity in field samples presents challenges when looking for correlations or developing models that describe fracture conductivity that are based on experiments performed with outcrop samples. While models can explain the behavior of samples of Indiana Limestone or San Andres Dolomite, no two field samples can be expected to show the same results. Moreover, the difficulty in using field rock experimentally without breaking the samples creates barriers in obtaining data experimentally. Figure 27 highlights this observation and compares the fracture conductivity of outcrop samples to field samples.

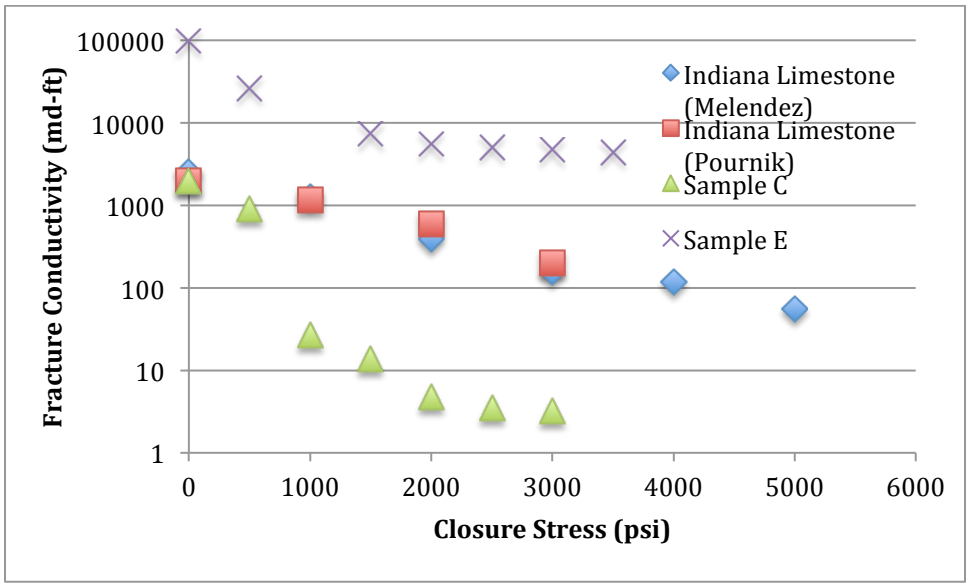

Figure 27: Fracture Conductivity Comparison of Outcrop and Field Samples

Figure 27 compares the fracture conductivity of two Indiana Limestone that were injected with 15% HCl for 15 minutes to Samples C and Sample E. Each sample listed in the figure was subjected to similar acid injection conditions and fracture conductivity

was measured over increasing values of closure stress. The Indiana Limestone samples were studied independently but exhibit very similar fracture conductivity. This is expected because the outcrop rock samples, as mentioned, exhibit significant homogeneity from sample to sample. However, Sample C and Sample E exhibit significantly different fracture conductivity behavior, despite being studied under the same conditions.

CHAPTER IV

CONCLUSIONS AND RECOMMENDATIONS

Conclusions

Six rock samples, labeled Samples A-F, were tested with 15% HCl. The data resulting from acid injection, fracture conductivity, and information from SEM-EDX analysis provided valuable insight into the interaction of 15% HCl and the rock samples. The following conclusions can be made based on the results of the research presented in this thesis.

1. SEM-EDX analysis revealed that the rock samples are made up of two regions, a carbonate dark region and an aluminosilicate light region. The lighter silicate region is more prevalent in each of the samples and will be chemically less sensitive to HCl
2. Acid injection appears to have the most impact on samples that have a higher acid solubility. Before and after pictures of each samples reveal the extent of rock dissolution in the presence of 15% HCl.
3. Fracture conductivity after acid injection does not seem to directly correlate with acid solubility. Fracture conductivity does correlate with the values of cumulative leak-off volume collected during the acid injection. The conclusion can be made that inherent rock matrix permeability explains the difference in fracture conductivity in each sample.
4. Measuring the fracture conductivity before and after introducing a chelating agent to Sample D determined that the fracture conductivity greatly increased. Coupled with the results of SEM-EDX analysis, it is concluded the chelating agent is a better agent

for improving fracture conductivity due to the increased amounts of aluminosilicates in the rock samples. Additional research on the effects of chelating agent on rock samples should be performed.

5. Based on the fracture conductivity results and the apparent etching of the fracture surfaces after acid injection, acid fracturing with 15% HCl is not recommended on rock that has an acid solubility less than 50 percent. Acid Fracturing is recommended on rock with an acid solubility greater than 50 percent.
6. Increased heterogeneity and the presence of hydrocarbons in the pore spaces of field rock samples present unique experimental challenges that are not present in outcrop rock samples. Future research should be directed at addressing these challenges.

Recommendations

The research presented in this thesis offers several pieces of information to assist in well stimulation strategies. However, additional research can be performed to get a greater understanding of the best strategy to stimulate the reservoir from which Samples A-F are collected. Given the high content of aluminosilicates present in the rock samples, additional tests using either chelating agent or alternative acid system should be performed. Alternative acid systems could include changing the concentration of HCl, 28% for example, in an effort to dissolve a greater amount of the carbonate regions of the rock samples. Another approach is to use a combination of HCl and hydrofluoric acid (HF), which is effective at dissolving silicates.

The acid injection apparatus is subject to corrosion when flowing 15% HCl. Future research should consider using a corrosion inhibitor to preserve the integrity of

the tubing, pressure transducers, and fittings used in the experiment. Additionally, the heating system for injection fluid should be modified to increase the heating capability of the system. Using the submersible heaters to preheat the KCl solution proved to be time consuming and removal from the process would decrease distractions during the injection. Finally, considerations should be made to replace the modified API cell. The fit of the silicone-covered samples inside the cell has diminished with successive experiments. While the use of Teflon tape and vacuum grease offers some seal to account for this discrepancy, a new cell could ideally fix some of the problems of fluids leaking around the samples.

REFERENCES

Abass, H.H., Al-Mulhem, A.A., and Mirajuddin, K.R. Acid Fracturing or Proppant Fracturing in Carbonate Formation? A Rock Mechanic's View. Paper SPE 102590 presented at the 2006 SPE Annual Technical Conference and Exhibition, San Antonio, Texas, 24-27 September.

Black, Harold N., and W. E. Hower. Advantageous Use of Potassium Chloride Water for Fracturing Water-Sensitive Formations. In *Drilling and Production Practice* (1965).

Crowe, C. W., R. C. Martin, and A. M. Michaelis. Evaluation of Acid-gelling Agents for Use in Well Stimulation. *SPE Journal* 21, no. 4 (1981): 415–424.

Economides, M.J., Hill, A.D., Zhu, D., Ehlig-Economides, C. et Al. 2012. *Petroleum Production Systems 2nd Edition.* Upper Saddle Ridge, New Jersey: Prentice Hall.

Gdanski, R. Kinetics of the Primary Reaction of HF on Alumino-Silicates. *Old Production & Facilities* 15, no. 4 (2000): 279–287.

Hendrickson, A. R., Hurst, R. E. and Wieland, D. R. Engineered Guide for Planning Acidizing Treatments Based on Specific Reservoir Characteristics. *Transactions,* AIME (1960): 219, 16.

Hensen, Emiel J. M., and Berend Smit. Why Clays Swell. *The Journal of Physical Chemistry B* 106, no. 49 (2002): 12664–12667.

Lund, K., Fogler, H.S., McCune, C.C., et al. 1975. Acidization-II. The Dissolution of Calcite in Hydrochloric Acid. *Chemical Engineering Science 30,* no. 8 (1975)**:**

825-835.

Mahmoud et al. 2010. Evaluation of a New Environmentally Firendly Chelating Agent for High Temperature Applications. Paper SPE 127923. Presented at the 2010 SPE International Symposium on Formation Damage Control. Lafayette, Louisiana. 10-12 February.

Malagon, C.: "The Texture of Acidized Fracture Surfaces-Implications for Acid Fracture Conductivity," M.S. Thesis, Texas A&M University, College Station, Texas (December 2006).

Melendez, M.G. 2007b. The Effects of Acid Contact Time and Rock Surfaces on Acid Fracture Conductivity. MS Thesis, Texas A&M University, College Station, Texas (August 2007).

Mukherjee, Hermanta, and Greg Cudney. Extension of Acid Fracture Penetration by Drastic Fluid-loss Control. *Journal of Petroleum Technology* 45, no. 2 (1993): 102–105.

Navarrete, R. C., M. J. Miller, and J. E. Gordon. Laboratory and Theoretical Studies for Acid Fracture Stimulation Optimization. In *SPE Permian Basin Oil and Gas Recovery Conference*, 1998.

Nierode, D. E., and K. F. Kruk. An Evaluation of Acid Fluid Loss Additives Retarded Acids, and Acidized Fracture Conductivity. In *Fall Meeting of the Society of Petroleum Engineers of AIME*, 1973.

O'Brien, Dennis, and Martin Chenevert. Stabilizing Sensitive Shales with Inhibited, Potassium-based Drilling Fluids. *Journal of Petroleum Technology* 25, no. 9 (1973): 1089–1100.

Pournik, Maysam. 2008. Laboratory-Scale Fracture Conductivity Created by Acid Etching. PhD dissertation, Texas A&M University, College Station, Texas (December 2008).

Williams, B.B., and Nierode, D.E. Design of Acid Fracturing Treatments. In *Transactions of the Society of Petroleum Engineers*, Vol. 253. Richardson Texas: Society of Petroleum Engineers.

Zou, C.L. Development and Testing of an Advanced Acid Fracture Conductivity Apparatus. M.S. Thesis, Texas A&M University, College Station, Texas (2005).

APPENDIX A

PHOTOGRAPHS BEFORE AND AFTER ACID INJECTION

Sample A

Before

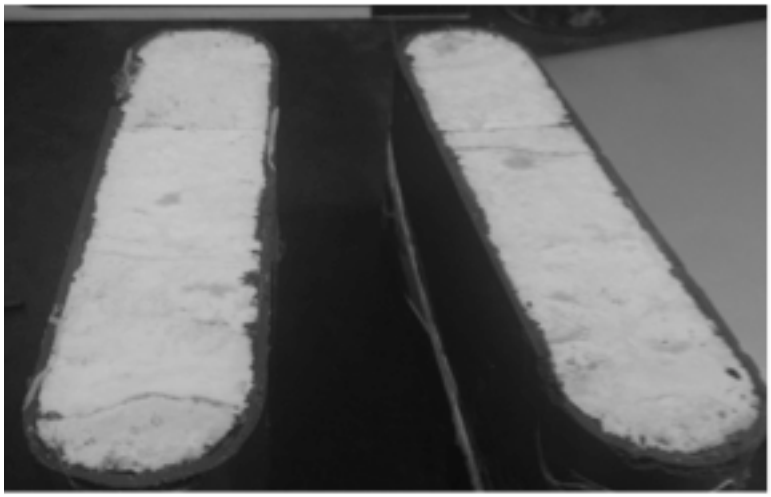

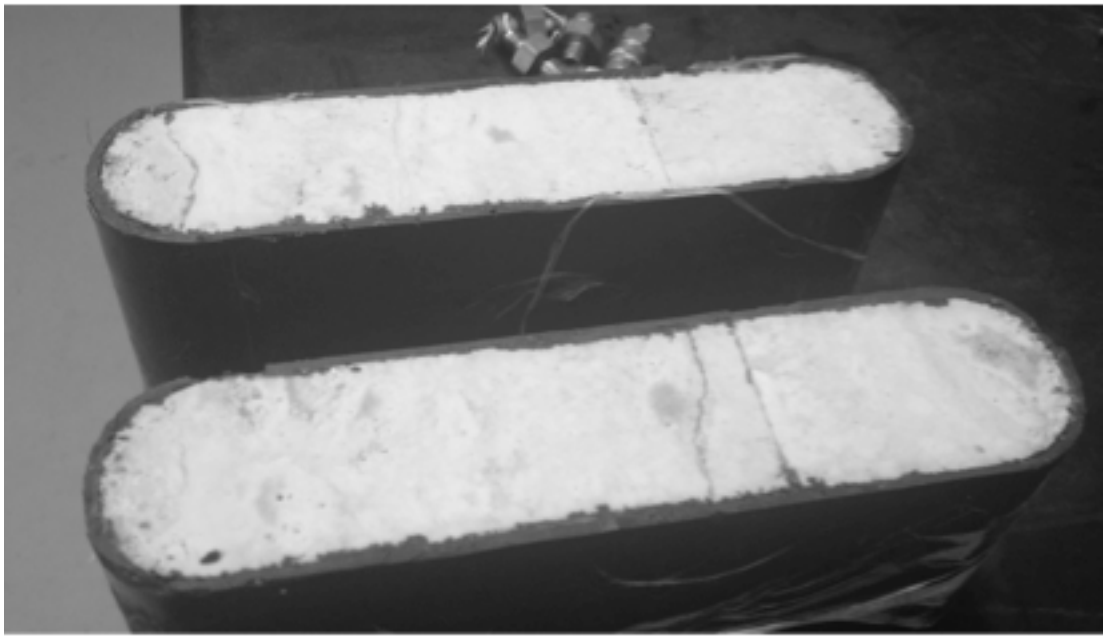

After

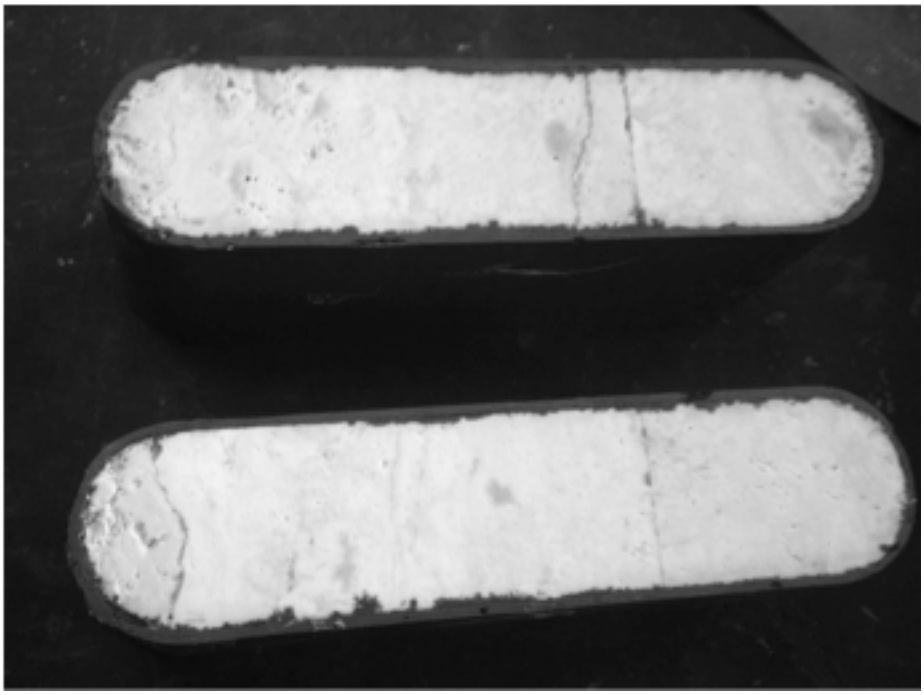

Sample B

Before

After

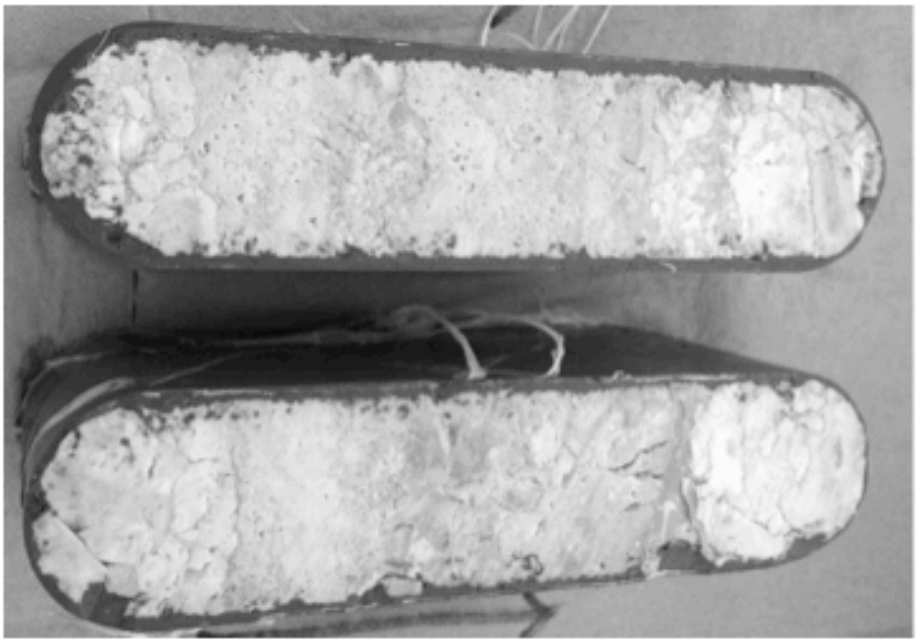

Sample C

Before

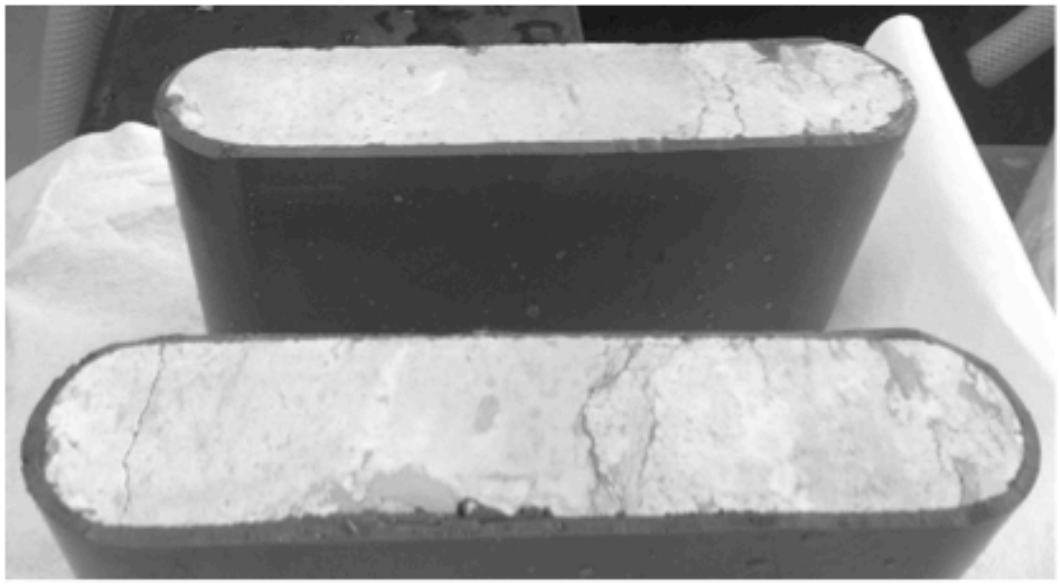

After

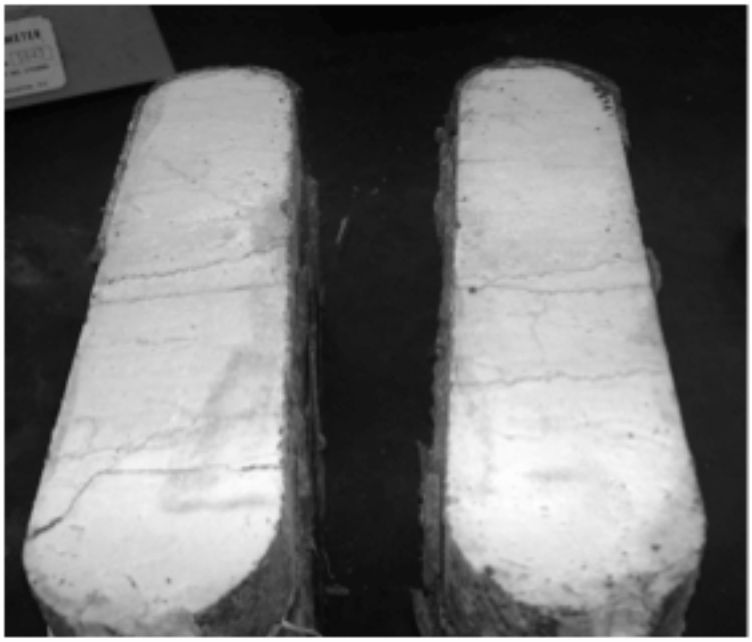

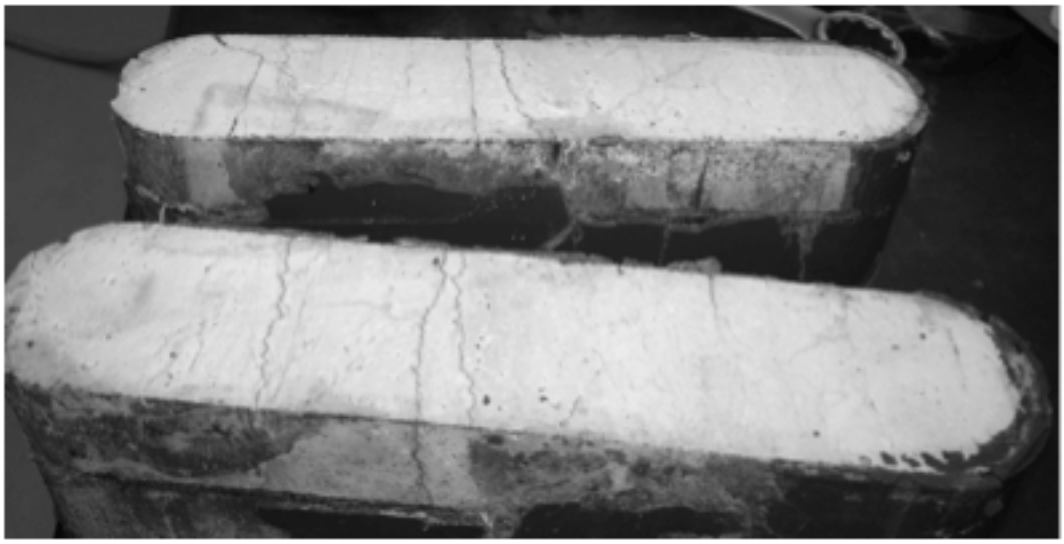

Sample D

Before

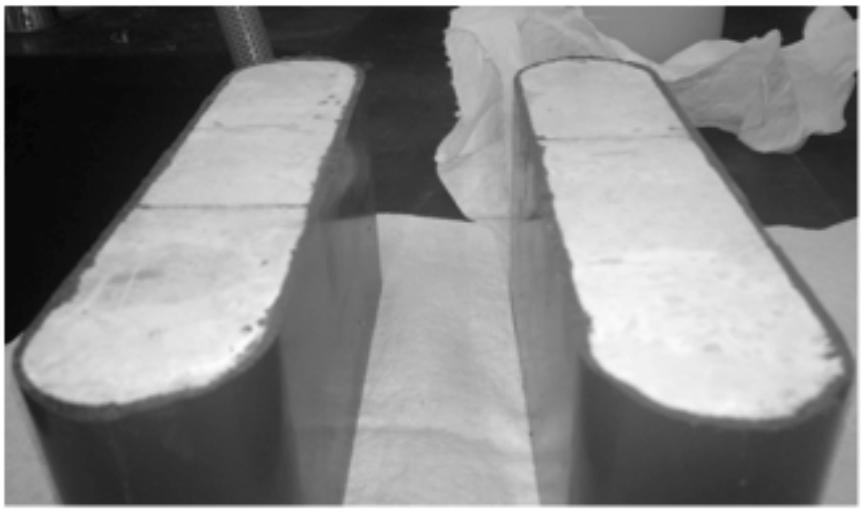

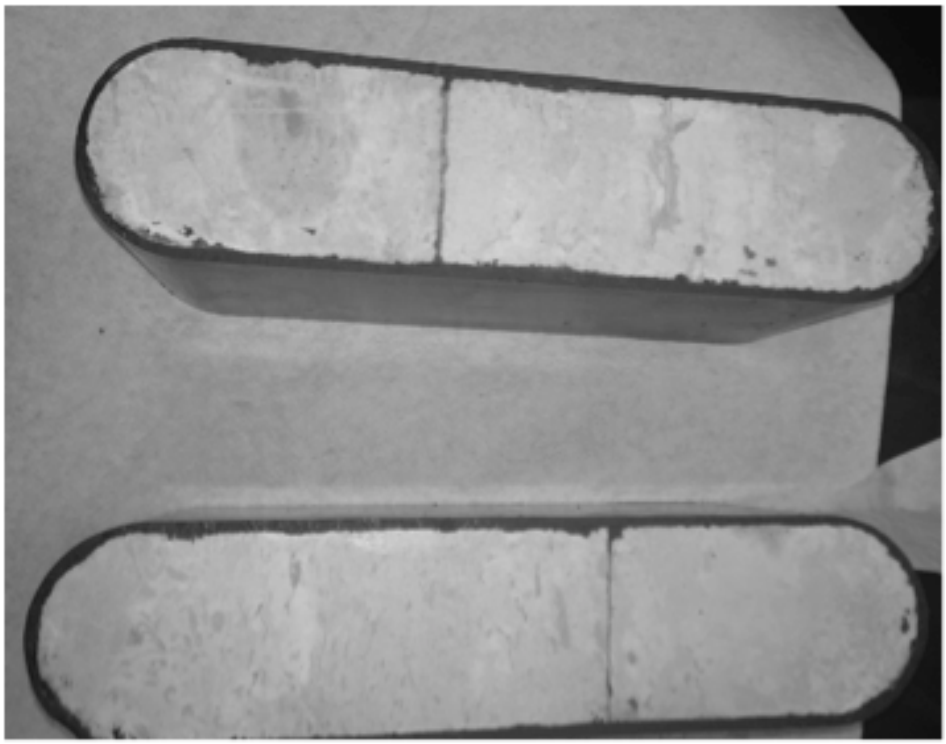

After

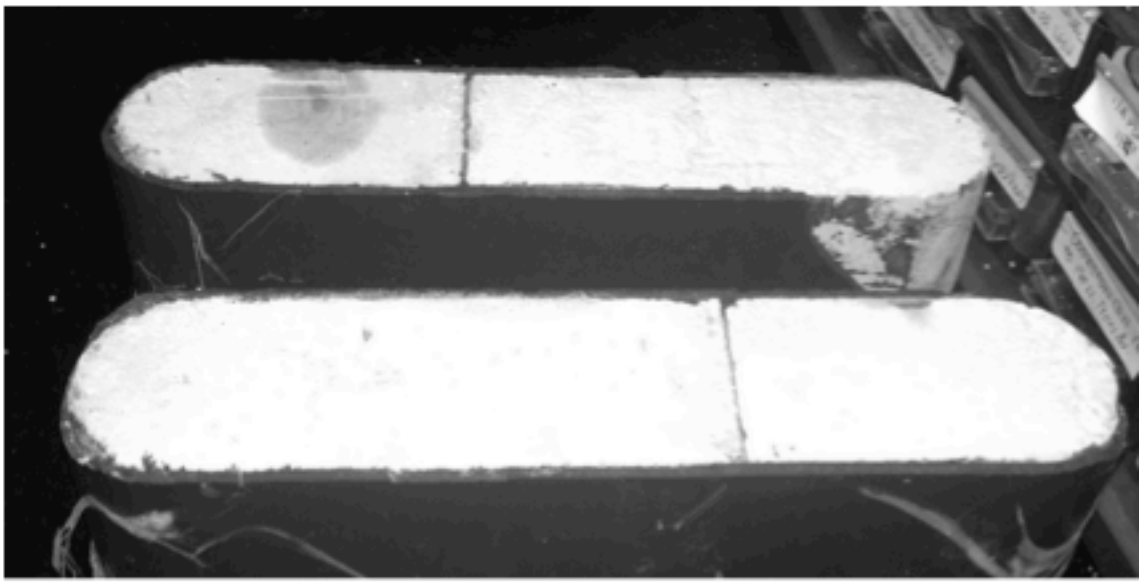

Sample E

Before

After

Sample F

Before

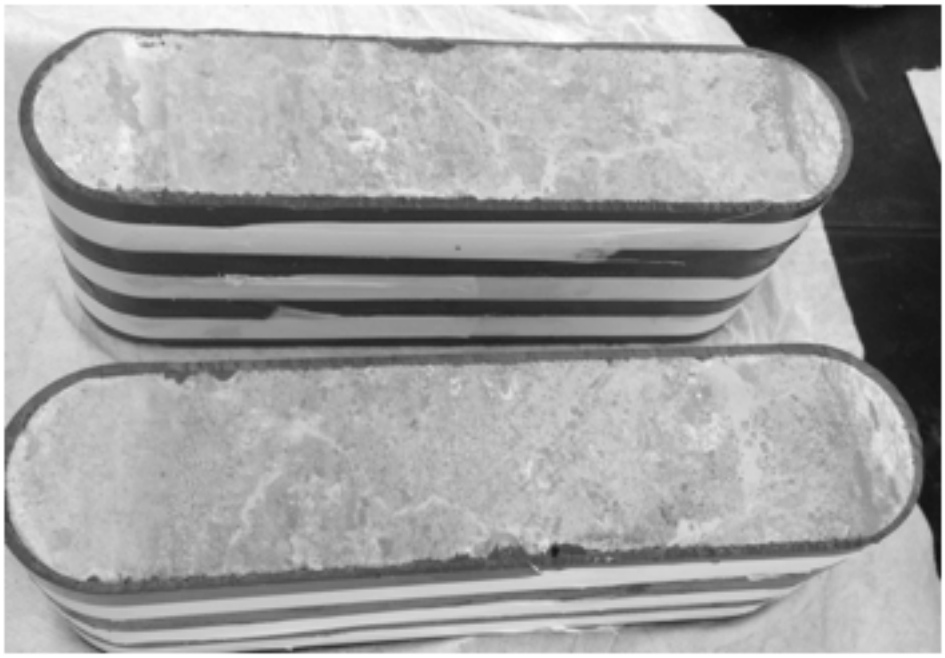

After

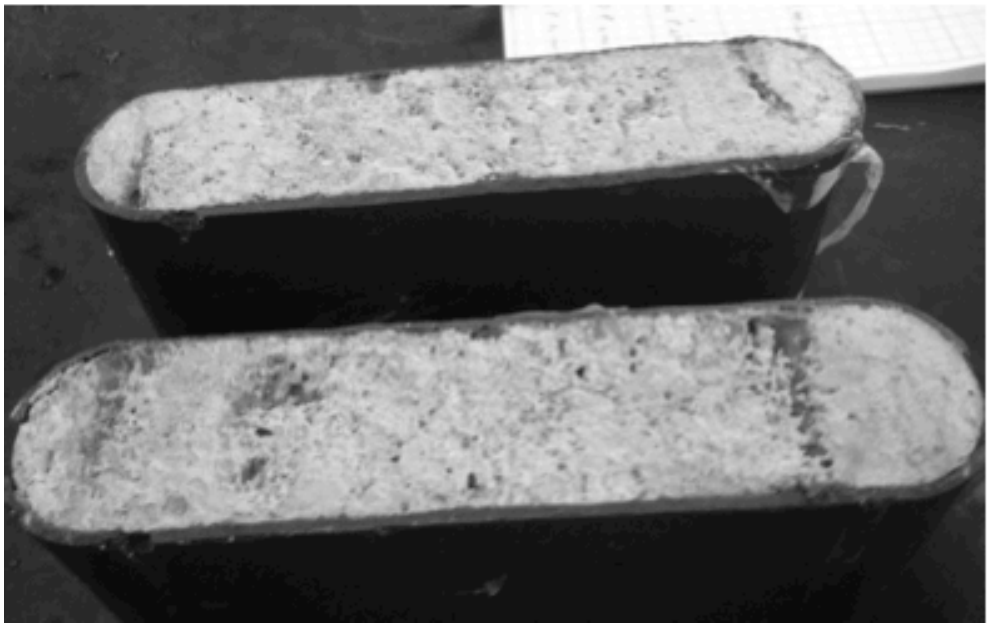

APPENDIX B

ACID FRACTURING SUPPLY LIST

Acid Fracturing Lab Supplies

	Vender Product Number	Vender
Tubing:		
1/2 inch 316 Steel	89785K55	McMaster-Carr
1/8 inch 316 Steel	89785K13	McMaster-Carr
O-rings:		
Cell 251-VT90	9464K551	McMaster-Carr
Caps 123-VT90	9464K87	McMaster-Carr
Pistons 351-VT90	8297T374	McMaster-Carr
Hoses		
Acid Reservoir to "T":	5238K768	McMaster Carr
Water Reservoir to "T":	5238K768	McMaster Carr
"T" to Pump:	5238K768	McMaster Carr
Pump to Heating Coils:	4468K814	McMaster Carr
Heating Coils to Cell :	4468K814	McMaster Carr
Discharge Line:	52375K14	McMaster Carr
Chemicals		
Silicone Primer (1 pint)	SS4155	RS Hughes
Silicone Kit	RTV-627	RS Hughes
Molykote Release Spray	4328T57	McMaster Carr
Vacuum Grease	2966K52	McMaster Carr
O-Ring Grease	1325K54	McMaster Carr
Casting Resin		Delvie's Plastics Inc

Temperature Probe	39095K95	McMaster Carr
Litmus Paper Roll	1434T31	McMaster Carr
Respirator (Medium)	4JG18	Grainger
Respirator (Large)	4JG19	Grainger
Cartridge	4JG12	Grainger

Wrenches Required:

7/8" in
9/16" in
7/16" in
5/16" in

Swagelok Fittings

1/16"	Temperature Gauge
1/8"	Pressure port lines
1/2"	Main Flow lines

APPENDIX C

DATA SHEETS

Sample A

Sample A Acid Injection			
Time (min)	T1(F)	T2(F)	Leak-Off Volume (mL)
0	135	135	0
1	126.3	129	14
2	121	125	30
3	119.7	122	45
4	118.4	120	65
5	117.8	119	85
6	117	118	109
7	116.8	117	126
8	116.6	117	146
9	116.4	117	174
10	115.7	116	196
11	116.2	116	217
12	115.2	116	241
13	115.2	116	260
14	114.5	115	278
15	114.7	115	292

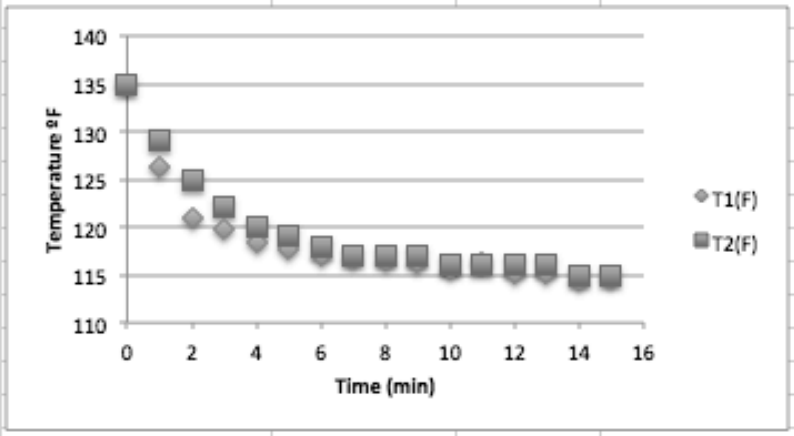

Temperature	135 F
Contact Time	15 min
Injection Rate	1 L/min
Addiitives	2% KCl
Acid	15% HCl

Sample A Conductivity			
Closure Stress (psi)	Fracture Conductivity (md-ft)		
0	-		
550	-		
1000	-		
1500	44.4562584		
2000	10.41574489		
2500	5.00527814		
3000	2.790757964		
3500	1.413329256		
4000	1.05232844		

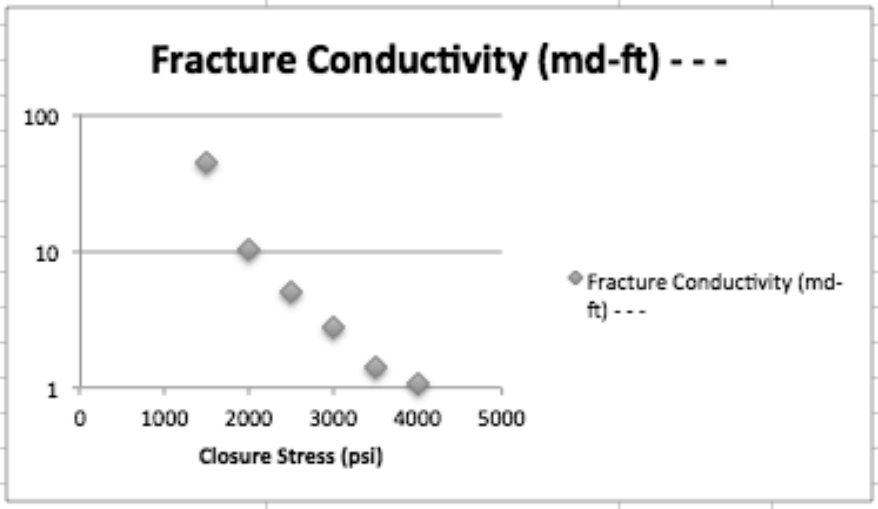

Sample B

Sample B Acid Injection				
Time (min)	T1(F)	T2(F)	Leak-Off Volume (mL)	
0	133.8	128	0	
1	125.7	127	16	
2	122.9	125	31	
3	121.0	122	43.2	
4	119.9	121	56.2	
5	119.0	119	67.8	
6	118.9	119	77.6	
7	117.5	118	86.6	
8	117.1	118	98.8	
9	116.6	118	113.3	
10	116.0	118	128.3	
11	115.4	118	151.3	
12	114.7	117	172.3	
13	115.0	117	187.3	
14	114.5	117	206.1	
15	114.3	117	320.4	

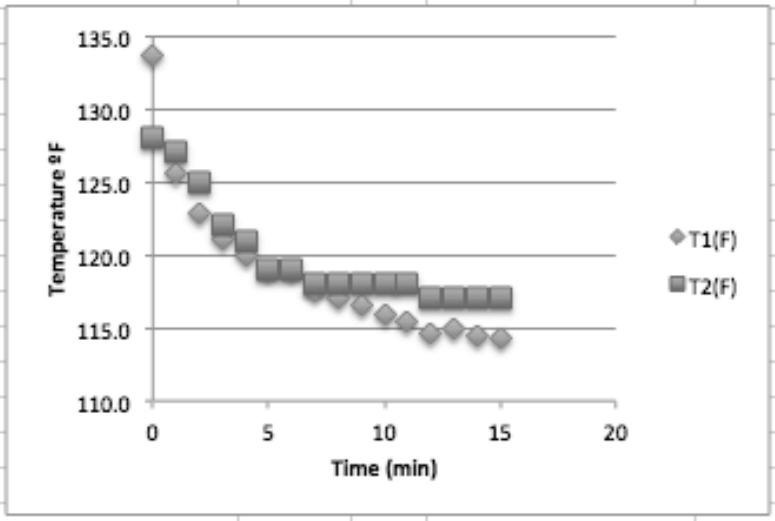

Temperature	135 F		*Leaks in fracture conductivity
Contact Time	15 min		prevented results
Injection Rate	1 L/min		
Addiitives	2% KCl		
Acid	15% HCl		

Sample C

Sample C Acid Injection			
Time (min)	T1(F)	T2(F)	Leak-Off Volume (mL)
0	135	135	0
1	121	126	10
2	121	125	18
3	119.5	124	24
4	118.8	123	32
5	118.05	123	39
6	117.24	122	46
7	116.43	122	53
8	115.62	122	61
9	114.81	123	68
10	114	122	75
11	113.19	123	82
12	112.38	123	89
13			
14			
15			

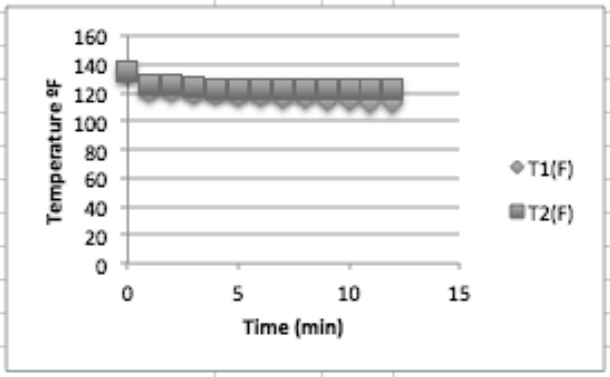

Temperature	135 F	*O-ring failure resulted in
Contact Time	15 min	stopping injection at 12 mintues.
Injection Rate	1 L/min	
Addiitives	2% KCl	
Acid	15% HCl	

Sample C Fracture Conductivity	
Closure Stress (psi)	Fracture Conductivity (md-ft)
0	1971
550	902
1000	26.5
1500	13.6
2000	4.8
2500	3.44
3000	3.23
3500	
4000	
4500	
5000	

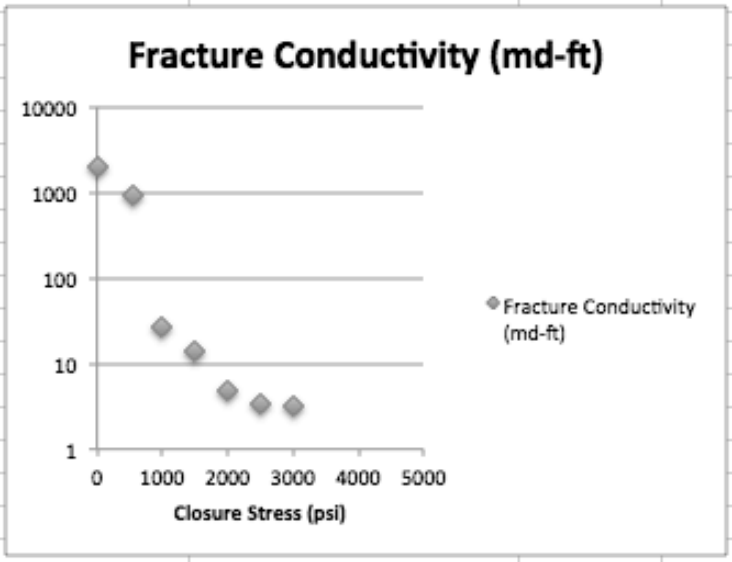

Sample D

Sample D Acid Injection				
Time (min)	T1(F)	T2(F)	Leak-Off Volume (mL)	
0	135	135	0	
1	135	135		
2	133	127	11	
3	132	120	15	
4	131	123	19	
5	129.5	114	24	
6	128.2	113	27	
7	126.9	111	28	
8	125.6	111	32.5	
9	124.3	111	37	
10	123	110	41	
11	121.7	110	45	
12	120.4	110	47.5	
13	119.1	109	50	
14	117.8	108	51.5	
15	116.5	109	52	

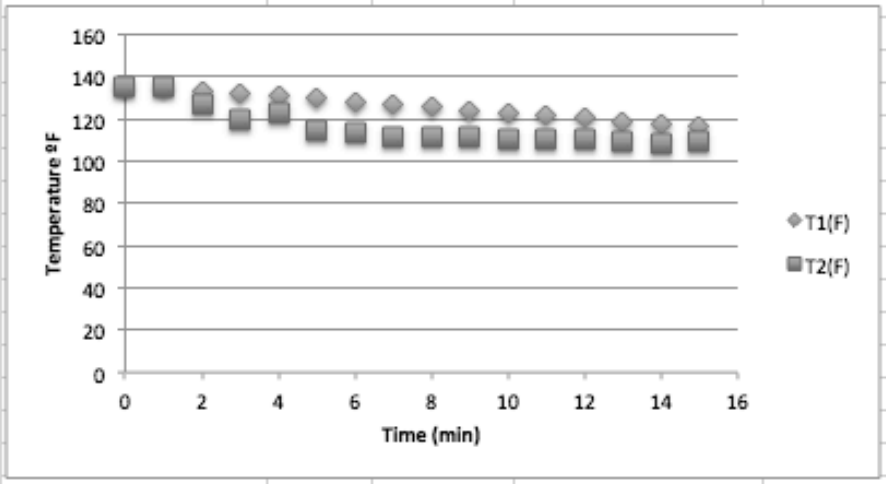

Temperature	135 F			
Contact Time	15 min			
Injection Rate	1 L/min			
Addiitives	2% KCl			
Acid	15% HCl			

Sample D Fracture Conductivity		
Closure Stress (psi)	Fracture Conductivity (md-ft)	After Chelating Agent (md-ft)
0	1971	7490.667316
550	902	
1000	26.5	1344.404564
1500	13.6	994.3721208
2000	4.8	663.0336725
2500	3.44	483.6463315
3000	3.23	329.3415376
3500		269.20697
4000		
4500		81.51381459
5000		55.98731014

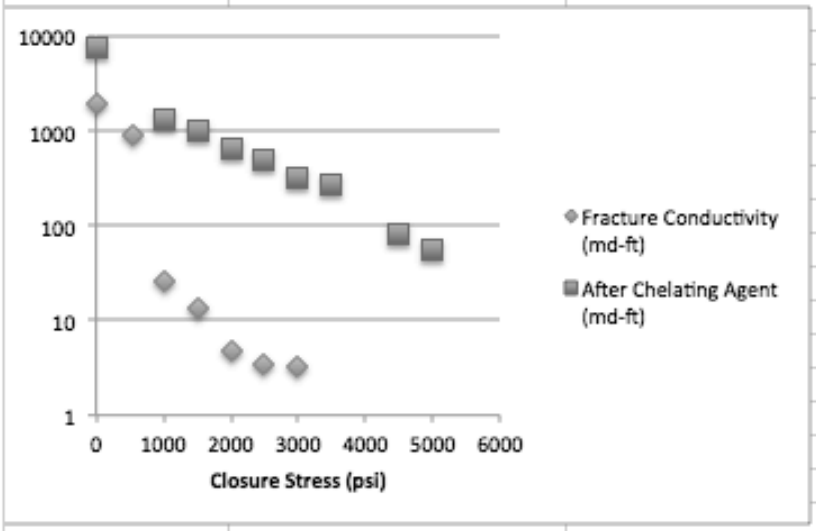

Sample E

Sample E Acid Injection				
Time (min)	T1 (F)	T2(F)	Leak-Off Volume (mL)	
0	135	133	0	
1	125	132	265	
2	122	126	470	
3	119	123	755	
4	118	122	1090	
5	117	120	1415	
6	119		1715	
7	116.6	119	2085	
8	116	118	2380	
9	116	117	2710	
10	116	117	3020	
11	115	117	3360	
12		117	3555	
13		117	3855	
14	115.2	117	4055	
15	115	116	4345	

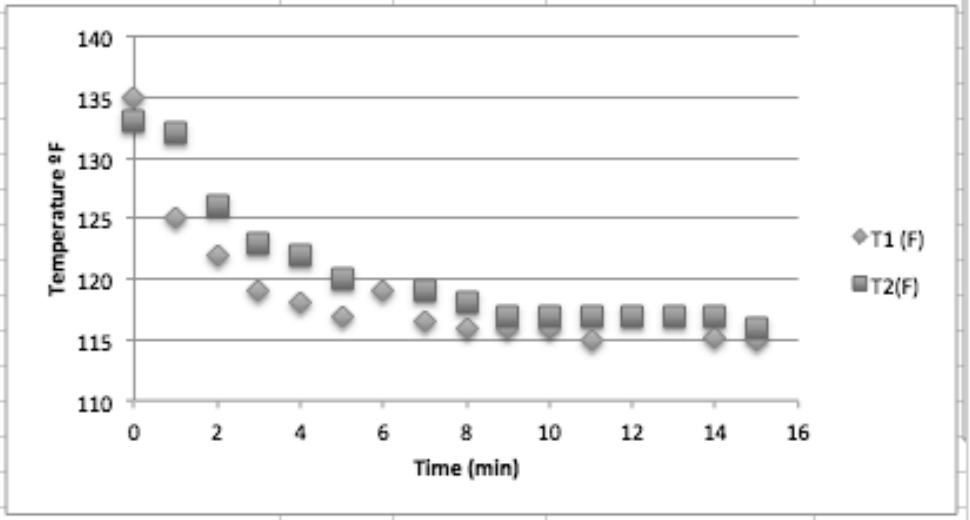

Temperature	135 F			
Contact Time	15 min			
Injection Rate	1 L/min			
Addiitives	2% KCl			
Acid	15% HCl			

Sample E Fracture Conductivity	
Closure Stress (psi)	Fracture Conductivity (md-ft)
0	99292.89951
550	26357.77258
1000	-
1500	7431.696564
2000	5541.047293
2500	5039.939039
3000	4703.178727
3500	4420.243423
4000	

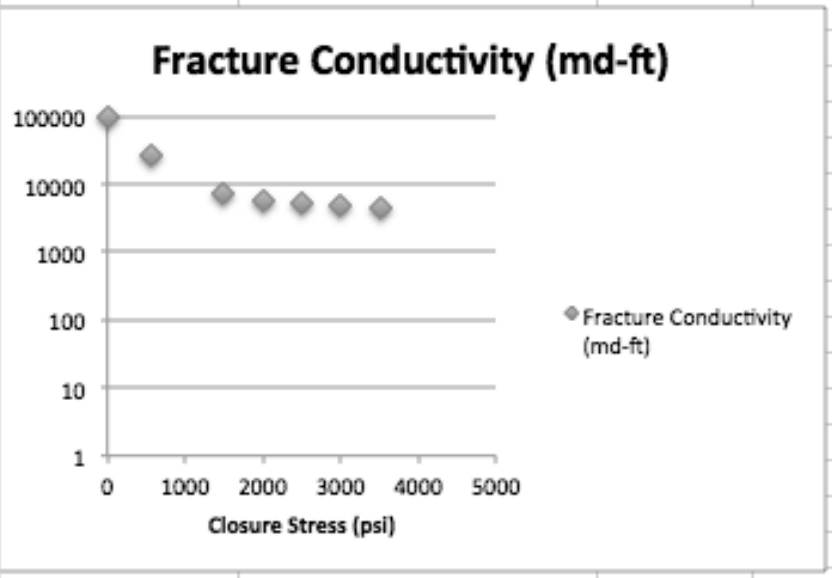

Sample F

Sample F Acid Injection				
Time (min)	T1(F)	T2(F)	Leak-Off Volume (mL)	
0	130	135	0	
1	121	126		
2	117.3	122	100	
3	115	123	150	
4	113.5	117	184	
5	112.7	116	247.5	
6	113.2	117		
7	111	114	380	
8	111.6	113	430	
9	111.4	113	495	
10	111.1	113	575	
11	111	112	620	
12	110.8	112		
13	110.6	112	715	
14	110.6	112	747	
15	111	113	775	

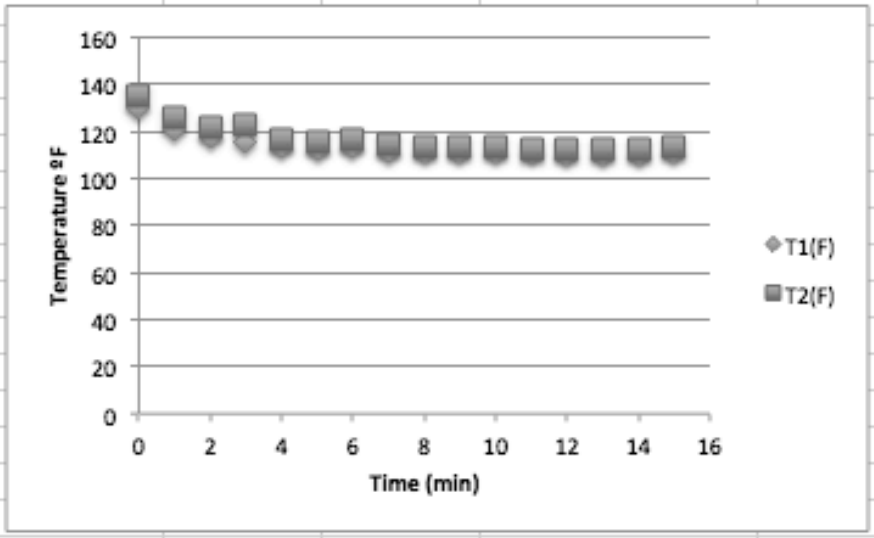

Temperature	135 F			
Contact Time	15 min			
Injection Rate	1 L/min			
Addiitives	2% KCl			
Acid	15% HCl			

Sample F Fracture Conductivity	
Closure Stress (psi)	Fracture Conductivity (md-ft)
0	2304.599891
550	280.4610764
1000	251.7473139
1500	188.1572069
2000	187.4028224
2500	161.860924
3000	136.4622592
3500	120.0429181
4000	105.0058072
4500	91.3634026
5000	80.13954898
5500	64.49247434
6000	53.08467039
6250	52.69493669